JVI Journals.ASM.org

High-Affinity Rb Binding, p53 Inhibition, Subcellular Localization, and Transformation by Wild-Type or Tumor-Derived Shortened Merkel Cell Polyomavirus Large T Antigens

Sophie Borchert,[a,b] Manja Czech-Sioli,[a] Friederike Neumann,[a] Claudia Schmidt,[a] Peter Wimmer,[b] Thomas Dobner,[b] Adam Grundhoff,[b] Nicole Fischer[a]

Institute for Medical Microbiology and Virology, University Medical Center Eppendorf, Hamburg, Germany[a]; Heinrich Pette Institute, Leibniz Institute for Experimental Virology, Hamburg, Germany

ABSTRACT

Interference with tumor suppressor pathways by polyomavirus-encoded tumor antigens (T-Ags) can result in transformation. Consequently, it is thought that T-Ags encoded by Merkel cell polyomavirus (MCPyV), a virus integrated in ~90% of all Merkel cell carcinoma (MCC) cases, are major contributors to tumorigenesis. The MCPyV large T-Ag (LT-Ag) has preserved the key functional domains present in all family members but has also acquired unique regions that flank the LxCxE motif. As these regions may mediate unique functions, or may modulate those shared with T-Ags of other polyomaviruses, functional studies of MCPyV T-Ags are required. Here, we have performed a comparative study of full-length or MCC-derived truncated LT-Ags with regard to their biochemical characteristics, their ability to bind to retinoblastoma (Rb) and p53 proteins, and their transforming potential. We provide evidence that full-length MCPyV LT-Ag may not directly bind to p53 but nevertheless can significantly reduce p53-dependent transcription in reporter assays. Although early region expression constructs harboring either full-length or MCC-derived truncated LT-Ag genes can transform primary baby rat kidney cells, truncated LT-Ags do not bind to p53 or reduce p53-dependent transcription. Interestingly, shortened LT-Ags exhibit a very high binding affinity for Rb, as shown by coimmunoprecipitation and *in vitro* binding studies. Additionally, we show that truncated MCPyV LT-Ag proteins are expressed at higher levels than those for the wild-type protein and are able to partially relocalize Rb to the cytoplasm, indicating that truncated LT proteins may have gained additional features that distinguish them from the full-length protein.

IMPORTANCE

MCPyV is one of the 12 known polyomaviruses that naturally infect humans. Among these, it is of particular interest since it is the only human polyomavirus known to be involved in tumorigenesis. MCPyV is thought to be causally linked to MCC, a rare skin tumor. In these tumors, viral DNA is monoclonally integrated into the genome of the tumor cells in up to 90% of all MCC cases, and the integrated MCV genomes, furthermore, harbor signature mutations in the so-called early region that selectively abrogate viral replication while preserving cell cycle deregulating functions of the virus. This study describes comparative studies of early region T-Ag protein characteristics, their ability to bind to Rb and p53, and their transforming potential.

Merkel cell polyomavirus (MCPyV) is one of 12 human polyomaviruses (1, 2), and to date is the only human polyomavirus for which solid evidence of a causative role in tumorigenesis exists. The virus was identified in Merkel cell carcinoma (MCC), a rare form of skin cancer seen in elderly and immunosuppressed patients (3). The high frequency of MCPyV detection in 60 to 90% of all MCC cases (4–9), monoclonal integration of the viral DNA in the tumor cells of primary tumors as well as metastases, MCC-specific signature mutations in the viral genome, and constitutive expression of putative viral oncogenes within the tumor cells strongly suggest a causative role for the virus during MCC pathogenesis (3, 9, 10).

Although most polyomaviruses do not induce tumors in their natural host, many family members can induce transformation of cells *in vitro*, with some of these viruses also being able to induce tumors in experimental animal models. The transformation ability of polyomaviruses is intricately linked to the expression of the early viral antigens, which include the small and large T antigens (sT-Ags and LT-Ags, respectively). Several members of the family additionally encode a middle T antigen (MT-Ag). MT-Ags can likewise contribute to transformation and in some cases (e.g., mouse polyomavirus) even exhibit the majority of transformation capacity (11, 12). In many polyomaviruses, however, LT-Ag appears to be the major transforming factor. LT-Ag-dependent transformation has been extensively studied using simian virus 40 (SV40) as a model system (13). SV40 LT-Ag deregulates cell growth by a variety of mechanisms that include binding of Hsc70, retinoblastoma (Rb) proteins, and p53 and result in the release of E2F-DP (E2 promoter binding-protein dimerization partner) from hypophosphorylated Rb and inhibition of p53-mediated transcriptional activation. At least three conserved domains contribute to SV40 LT-Ag-induced transformation: the J domain and LxCxE motif, which are located in the in the N-terminal half of the protein and bind to Hsc70 and Rb proteins, respectively, and a p53

Received 4 October 2013 **Accepted** 20 December 2013

Published ahead of print 26 December 2013

Editor: M. J. Imperiale

Address correspondence to Nicole Fischer, nfischer@uke.de, or Adam Grundhoff, adam.grundhoff@hpi.uni-hamburg.de.

doi:10.1128/JVI.02916-13

binding domain located in the C terminus. The N terminus, including the J domain and the LxCxE motif, can be sufficient to transform cells *in vitro* (14). Similar to SV40 LT-Ag, the LT proteins encoded by the related JC and BK polyomaviruses have also been shown to induce transformation *in vitro*, although less efficiently than those of SV40 (15, 16). The lower transformation efficiency is a likely consequence of the reduced affinity with which these proteins bind to the Rb family of tumor suppressors (17).

Interestingly, all large tumor antigen (LT-Ag) sequences recovered from primary MCC tumors or tumor-derived cell lines harbor signature mutations that lead to the expression of shortened LT-Ag proteins. These truncation products unequivocally preserve the Rb binding motif, but they lack a functional origin binding domain (OBD) and ATPase/helicase region (10, 18, 19). It is thought that these truncations are the result of a selection pressure to abrogate untimely firing of viral origins from integrated viral genomes (9, 20). However, whether MCPyV LT-Ag is able to interfere with p53 and whether the truncation event would abrogate this ability are currently under discussion (21). Likewise, given that the coding regions for sT- and LT-Ags partially overlap, it is unclear whether retention of the LxCxE motif signifies an important role for LT-Ag-mediated Rb inactivation during MCC pathogenesis or, rather, reflects a requirement to preserve a functional sT gene. In several polyomaviruses, sT-Ags can complement the transforming and tumor-inducing functions of LT and MT (22–24). Indeed, Shuda and colleagues demonstrated that MCPyV sT-Ag is expressed in nearly all MCPyV-positive tumors and exhibits transforming potential in rat-1 cells, most likely through a mechanism that affects the phosphorylation status of 4E-BP1 (25). However, the fact that suppression of sT-Ag alone in sT- and LT-Ag-positive cell lines does not fully recapitulate a pan-T knockdown suggests a synergistic role of both T antigens during MCC tumorigenesis (25, 26). Additionally, it was recently demonstrated that sT-Ag contributes to LT-Ag expression by targeting the cellular ubiquitin ligase SCF(Fbw7), thereby preventing proteasomal degradation of LT-Ag (27).

Given the above, we have performed a side-by-side comparison of a consensus, full-length MCPyV LT-Ag (28) and several truncated LT protein genes from previously characterized MCC-derived cell lines (18). Here, we demonstrate the characterization of the encoded LT-Ag proteins with regard to their subcellular localization, steady-state expression, transformation potential, and capacity to bind to Rb and p53. All analyses were performed in comparison to the well-characterized SV40 LT-Ag protein. We show that full-length MCPyV LT-Ag does not directly bind to p53, but nevertheless can target the p53 pathway via an as-yet-unknown factor, thereby significantly reducing p53-dependent transcription. In contrast, tumor-derived truncated LT-Ags are unable to bind to p53 and do not affect p53-dependent transcription. Our results also demonstrate that tumor-derived truncated MCPyV LT-Ag proteins show elevated steady-state expression levels, bind with very high affinity to Rb, and can partially relocalize Rb to the cytoplasm, indicating that removal of the carboxy-terminal region not only abrogates viral replication and lowers growth inhibition (21, 29) but may also modulate other functions of MCPyV LT-Ag. We also provide statistical evidence suggesting that MCC-specific mutations positively select for the presence of the LT-Ag LxCxE motif, independently of the need to preserve the first exon shared with sT-Ag, and demonstrate transformation of primary baby rat kidney cells by early region constructs encoding full-length and truncated MCPyV LT genes. Collectively, our data support the hypothesis that truncated MCPyV LT-Ag plays an important role during the pathogenesis of MCC.

MATERIALS AND METHODS

Cell lines. 293 cells (30), H1299 cells (31), and Saos-2 cells (32) were grown as monolayer cultures in Dulbecco's modified Eagle's medium (DMEM) supplemented with 10% fetal calf serum (FCS) and 5% penicillin-streptomycin in a 5% CO_2 atmosphere at 37°C. PFSK-1 cells, WaGa cells, and MKL-1 cells were grown in RPMI medium supplemented with 10% FCS and 5% penicillin-streptomycin.

Plasmids and transient transfections. The MCPyV LT full-length expression construct (pCMV2b-MCPyVLT$_{FL}$) was generated by PCR amplification using a taqExpand PCR amplification system (Roche Diagnostics) and genomic DNA of a synthetic MCPyV clone (MCVSyn) as the template (28). pCMV2b-LT$_{MCCL-3}$, pCMV2b-LT$_{MCCL-11}$, and pCMV2b-LT$_{MCCL-12}$ were constructed by PCR amplification from genomic DNA of MCPyV-positive MCC cell lines (MCCL-3, -11, -12) (18). pCMV2b-LT$_{MCC350}$ was generated by PCR amplification using expression plasmid pCDNA-MCV350 (NIH AIDS Reagent Program). pCMV2b MCPyV LT expression constructs contain an N-terminal FLAG expression tag. The following PCR primers were used: MCPyV_XhoI_FL_R (where R indicates reverse), 5′-GGGCTCGAGTTGAGAAAAAGTACCAGAATCTTG; MCPyV EcoRV_F (where F indicates forward), 5′-CCGATATCATGGATTTAGTCCTAAATAGG; MCPyV_350_XhoI_R, 5′-GGGCTCGAGATCTGTAAACTGAGATGACGAGGC; MCCL-12_LT_XhoR, 5′-GGGCTCGAGGAATGGAGGAGGGGTCTTCGG; SV40ori_F, 5′-CCTCGAGAGCCTAGGCCTCCAAAAAAG; SV40_ori_R, 5′-CCTCGAGTCCGCCCCATGGCTGAC; MCPyV_ori_F, 5′-CCTCGAGCAAGGGCGGGAAAC; MCPyV_ori_R, 5′-CCTCGAGCTTGTCTATATGCAG; SV-YFP-N-F-XhoI, 5′-CTCAGATCTCGAGCTATGGATAAAGTTTTAAACAGAGAGG; SV-YFP-N-R-EcoRI, 5′-CAGAATTCTTATGTTTCAGGTTCAGGGGG; SV-YFP-C-F-NheI, 5′-CCGCTAGCATGGATAAAGTTTTAAACAGAGAGG; SV-YFP-C-R-AgeI, 5′-GACCGGTGCACCTGCTCCTG-TTTCAGGTTCAGGGGGAG; MCPyV YFP-N-F-BsrGI, 5′-CTGTACAAGGGAGCAGGTGCAGGAGCAATGGATTTAGTCCTAAATAGG; MCPyV YFP-N-R-NotI, 5′-GCGGCCGCTTATTGAGAAAAAGTACCAGAATC; MCPyV YFP-C-F-NheI, 5′-CCGCTAGCATGGATTTAGTCCTAAATAGGAAAG; MCPyV_YFP-C-R-AgeI, 5′-GACCGGTGCACCTGCTCCTTGAGAAAAAGTACCAGAATC; MCCL-11 YFP-N-R-NotI, 5′-CGCGGCCGCTTCATCTGGGCTGCCGGG; MCCL-11 YFP-C-R-AgeI, 5′-GACCGGTGCACCTGCTCCTCTGGGCTGCCGGGGCG. The SV40 LT cDNA containing plasmid pZIPTEX (33) was kindly provided by W. Deppert. pHCMV2-SV40LT$_{FL}$ encoding untagged full-length SV40 LT was generated by subcloning a BamHI fragment of pZIPTEX into pHCMV (34).

Luciferase expression plasmids containing E2F binding sites (pI-H2A-68) or mutated E2F binding sites (pI-H2A-68*) in the H2A promoter region together with cytomegalovirus (CMV) expression plasmids for Rb or E2F have been described before (35). Human adenovirus 5 (hAdV5) pcDNA3.1-E1B-55K has also been described previously (36). pC53-SN3 expresses human wild-type (wt) p53 from the pCMV/neo vector (37). The firefly luciferase reporter plasmid pRE-Luc contains five p53-binding sites upstream of a minimal cytomegalovirus promoter and was described before (38).

pCR2.1-MCPyVori was constructed by amplification of the 97-bp MCPyV replication origin (39) followed by ligation into the XhoI site of pCR2.1. For transient transfection of 293 cells and H1299 cells, 25-kDa linear polyethylenimine (Polysciences Inc., Eppelheim, Germany) was used as the transfection reagent (40). Saos-2 cells were transfected in the presence of FuGene (Roche).

Viral replication assays. Replication assays were performed with PFSK-1 cells. The cells were cotransfected with 1 μg of pCR2.1 ori plasmid and 1 μg of LT expression constructs for 48 or 96 h. Low-molecular-weight DNA was isolated according to the Hirt protocol as recently de-

scribed (28). Briefly, DNA was digested with DpnI to distinguish replicated DNA from input DNA and EcoRI for linearization. Digested DNA was resolved on a 1% agarose gel, transferred to Hybond-N+ (Amersham Pharmacia) membrane by Southern blotting, UV cross-linked, and hybridized overnight at 42°C with a ^{32}P-labeled probe (Rediprime II DNA labeling system, random-primed labeled; GE Healthcare) corresponding to the restriction fragment HinDIII/EcoRV (pCR2.1-MCPyVori).

Antibodies and Western blot analysis. For protein extraction, pelleted cells were resuspended in lysis buffer (50 mM Tris [pH 8.0], 150 mM NaCl, 1% NP-40, 0.5% Na-deoxycholate, 5 mM EDTA, 0.1% SDS). Proteins were separated by SDS-PAGE and blotted on a nitrocellulose membrane. Primary antibodies specific for polyomavirus proteins used in this study include MCPyV LT-Ag mouse monoclonal antibody (MAb) Cm2B4 (10) (Santa Cruz) and SV40 LT mouse MAb Pab419 (41). p53 mouse MAb DO-1, polyclonal Ab FL-393, Brd4 specific rabbit polyclonal Ab H-250, and Rb rabbit polyclonal Ab M-153 were purchased from Santa Cruz, and the FLAG-M2 used in immunoprecipitation studies was purchased from Sigma-Aldrich. Actin mouse MAb was applied in Western blot analyses to ensure loading of equal protein amounts (Chemicon catalog no. 1501). The secondary antibodies conjugated to horseradish peroxidase (HRP) for detection of proteins by immunoblotting were anti-mouse IgG (GE Healthcare) and anti-rabbit IgG (Santa Cruz).

pBRK cell transformation assay and anchorage-independent growth assay. Primary baby rat kidney (pBRK) cells were obtained from kidneys of 7-day-old Sprague-Dawley rats as previously described (42). Soft agar colony formation assay was performed according to published protocols (43).

Immunofluorescence staining and confocal microscopy. For indirect immunofluorescence, cells were grown on glass coverslips coated with 0.2% gelatin (Sigma). Cells were fixed in 4% paraformaldehyde in phosphate-buffered saline (PBS; 15 min) and permeabilized in PBS–1% Triton X-100 for 30 min. After 1 h of blocking in Ca^{2+}/Mg^{2+}-free PBS containing a buffer of 1% Triton X-100, 0.5% Tween, and 3% bovine serum albumin (BSA; albumin fraction), coverslips were treated for 1h with the primary antibody diluted in blocking buffer and washed in PBS–0.1% Tween 20, followed by incubation with the corresponding secondary antibodies (Dianova, Hamburg, Germany). Coverslips were mounted in Vectashield medium, and digital images were acquired with a confocal laser-scanning microscope (Leica DM IRE2 with a Leica TCS SP2 AOBS confocal point scanner) equipped with an oil-immersion Plan Apo ×63, numerical aperture (NA) 1.4 objective. Images were cropped using Adobe Photoshop CS5 and assembled with Microsoft PowerPoint.

Luciferase assay. For p53-dependent transcription using dual-luciferase assays, subconfluent H1299 cells were transfected in 24-well plates with a DNA/polyethyleneimine (PEI) mixture using the effector plasmids, pc53-SN (25 ng) and pRL-TK (250 ng) (Promega). Where necessary, empty pCMV2b vector was added such that the total amount of transfected DNA was 3.5 μg per sample across all experiments. Total-cell extracts were prepared 36 h after transfection in 1× lysis buffer, and luciferase activity was assayed with 20 μl of extract. All samples were normalized for transfection efficiency by measuring *Renilla* luciferase activity. All experiments were performed in triplicate.

For luciferase assays measuring Rb binding and E2F activation, 3×10^4 Saos-2 cells were transfected in 24-well plates using FuGene transfection reagents (Roche) with pI-H2A-68, CMV-Rb, and LT-Ag as indicated in the legend to Fig. 6. pRL-TK was cotransfected for normalization. At 36 h posttransfection, cell extracts were prepared and luciferase activity was determined using a dual-luciferase assay (Promega) according to the manufacturer's instructions.

Coimmunoprecipitation (co-IP) studies. Total-cell extracts were prepared by using lysis buffer (10 mM HEPES [pH 7.8], 10 mM KCl, 2 mM $MgCl_2$, 0.1 mM EDTA, 1% Nonidet P-40) supplemented with a protease inhibitor mixture (Roche). After 30 min on ice and cell disruption, 2 volumes of TN buffer (200 mM NaCl, 20 mM Tris supplemented with protease inhibitors) were added, and cell lysate was cleared by centrifugation (4°C, 14,000 rpm, 30 min). After normalizing for protein concentration, whole-cell extracts were subjected to immunoprecipitation. Supernatant was precleared by adding 35 μl protein A/G Sepharose (Santa Cruz) for 30 min at 4°C. A 10-μl antibody solution was added to the lysate, and the mixture was rotated at 4°C O/N. Thirty-five microliters of protein A/G Sepharose was added for 1 h at 4°C with rotation. Beads were washed 5× (TN buffer), and FLAG proteins were eluted from the beads by competition with the FLAG peptide (100 μg/ml) or by adding SDS loading buffer and with subsequent boiling of the samples.

FACS-FRET. Fluorescence-activated cell sorter–fluorescence resonance energy transfer (FACS-FRET) was performed as recently described (44) using the Clontech vectors pEYFP-C1/N1 and pECFP-C1/N1. Merkel cell polyomavirus sequences were N- and C-terminally tagged using the pEYFP-N1 vector and the restriction sites NheI/AgeI and BsrGI/NotI, respectively. Tagged SV40 LT-Ag was generated using the pEYFP-C1 vector with restriction sites NheI/AgeI for N-terminal tagging and the vector pECFP-C1 with XhoI/EcoRI sites for C-terminal tagging. The positive control for FACS-FRET (cyan fluorescent protein [CFP]-fused yellow fluorescent protein [YFP]) was kindly provided by M. Schindler (44). pEYFP p53 and pECFP p53 plasmids were provided by W. Ching, Heinrich Pette Institute, Hamburg.

Quantitative RT-PCR. Total RNA from three independent experiments was isolated from PFSK-1 or U2OS cells at 48 h posttransfection using an RNeasy Mini Kit and column DNase I digestion. One hundred nanograms of total RNA was used in a one-step reverse transcription-PCR (RT-PCR; Thermo Scientific) using gene-specific primers in a 10-μl volume of reaction mixture. Primer sequences for p21, Hdm2, GADD45A, cdc2, cyclA2, glyceraldehyde-3-phosphate dehydrogenase (GAPDH), and RLP13 have been published previously (29, 45, 46).

Cycling was performed using a Rotor-Gene Q-plex (Qiagen) at the following conditions: 5 min at 95°C, 40 cycles of 15 s at 95°C, 20 s at 60°C, and 15 s at 72°C, followed by melting curve analysis. The data were analyzed using Rotor-Gene software, and mRNA of each gene was normalized to two housekeeping mRNA levels, those of GAPDH and RLP13.

Cell fractionation. To fractionate cells into cytoplasm and nuclei, cells were resuspended in 10 mM HEPES [pH 7.9], 1.5 ml $MgCl_2$, 10 mM KCl, and 0.5 mM dithiothreitol (DTT) and incubated on ice for 5 min. Cells were disrupted using a Dounce homogenizer. The cytoplasmic fraction was separated from nuclei and other components by centrifugation at 228 × *g* at 4°C for 5 min. To isolate nuclei, the nuclear pellet was resuspended in 0.25 M sucrose–10 mM $MgCl_2$ and centrifuged for 10 min at 2,800 × *g* at 4°C through a sucrose cushion containing 0.88 M sucrose and 0.5 mM $MgCl_2$. The method used to fractionate cells into the cytoplasm, nucleoplasm, nuclear membrane, chromatin, and extracellular matrix was published earlier (47).

Bacterial expression and purification of N-terminal LT proteins and the Rb pocket domain. Coding sequences for truncated SV40 LT_{7-117} and MCPyV LT_{1-244} were PCR amplified using pZIPTEX (33) or cDNA from the MCPyV-positive MCC cell line 12 (18) as the template, and PCR fragments were sequenced and subcloned into pRSETA (Invitrogen). N-terminal His-tagged proteins were expressed in BL21 Star in LB medium supplemented with 1% glucose at 37°C for 4 h using 1 mM isopropyl-β-D-thiogalactopyranoside (IPTG; for SV40 LT) or at 16°C for 18 h using 0.5 mM IPTG (for MCPyV LT). Ni-nitrilotriacetic acid (Ni-NTA) purification was performed with 50 mM Tris [pH 7.5], 150 mM NaCl (750 mM NaCl for MCPyV LT), 5% glycerol, and 1 mM DTT (5 mM β-mercaptoethanol for MCPyV LT). Proteins were eluted using an imidazole gradient of 20 to 500 mM imidazole. Size exclusion chromatography was executed under the same buffer conditions with an Äkta Prime Superdex 200. Fractions containing monomeric LT protein were pooled, dialyzed, and concentrated. Rb sequences encoding to the pocket domain (amino acids [aa]382 to 771) were subcloned into the glutathione *S*-transferase (GST) expression plasmid pGEX4T3. Bacterial expression was performed with BL21 Star grown in LB medium supplemented with 1% glucose, protein

expression was induced with 0.5 mM IPTG, and cells were grown at 16°C for 18 h. The purification strategy has been described before (48).

MST. The microscale thermophoresis (MST) background has been reviewed recently (49). The dissociation constant of bacterially expressed N-terminally truncated LT proteins binding to the purified Rb pocket domain was measured using a Monolith NT115 (NanoTemper). Purified Rb pocket domain fragments were Alexa 647 labeled by following the manufacturer's protocol. A solution of monomeric LT proteins was serially diluted as indicated in Results. The labeled Rb pocket domain was incubated with the LT protein dilutions at room temperature in the dark for 30 min. Measurements were performed with 50 mM Tris [pH 7.4], 0.05% Tween [150 mM], and 200 mM or 250 mM NaCl at 50% red light-emitting diode (LED) power and 60% infrared (IR) laser power using hydrophilic capillaries. Measurements were also carried out at 20% and 40% IR laser power. Three independent measurements at the conditions described in Results were executed. Data analysis was performed using NanoTemper analysis software. Curves were fitted using nonlinear regression Hill slope (GraphPad Prism).

Statistical analysis of MCC-derived MCPyV LT-Ag genes. In addition to three truncated LT-Ag genes analyzed in one of our earlier studies, we extracted all annotated MCPyV LT-Ag coding sequences deposited in the NCBI database as of 15 January 2013 ($n = 148$). After multiple nucleotide sequence alignments, we identified all MCC-derived entries that contain a truncating mutation and eliminated all duplicate entries, leaving 40 unique entries for further analysis (detailed information is available upon request). For amino acids encoded by the second exon (the first exon must be considered fixed, since it is shared with sT-Ag), we next calculated *P* values for the hypothesis that this position is subject to positive or negative selection during MCC pathogenesis. For negative selection of amino acids located between the first observed truncation site and the last amino acid encoded by the second exon, the probability of the corresponding null hypothesis is given by the accumulated binomial probability that exactly the observed number of or more truncation events occur before the given position. Conversely, for positive selection of amino acids between the first amino acid encoded by the second exon and the last observed truncation site, the probability of the null hypothesis corresponds to the accumulated probability that exactly the observed number of or more truncation events occur after the position in question. The amino acid positions at which the significance of the calculated *P* values was maximal were then considered to be most likely to signify the position at which positive or negative selection, respectively, occurs.

RESULTS

MCC-derived truncated LT-Ags show highly significant selection for the presence of the LxCxE motif. All known MCC-derived truncated LT-Ag (tLT-Ag) harbor mutations that lead to the removal of the C-terminal helicase/ATPase domain, presumably due to a selection pressure to abrogate untimely firing of viral origins (9, 20). It is also notable that the truncating mutations unequivocally occur downstream of the LxCxE motif, an observation which would seem to suggest an important role for tLT-Ag-mediated Rb inactivation during MCC pathogenesis. Yet, given that LT- and sT-Ag share their first exon, one could also argue that the above may predominantly reflect a requirement to preserve a functional sT-Ag gene.

Indeed, only 60 nucleotides (nt) separate the LxCxE coding sequences from the 5′ end of the second exon in the SV40 LT-Ag gene. However, the MCPyV LT-Ag gene additionally encodes a unique 118-aa-long serine-rich region of unknown function (Fig. 1A, U1 region) and thus offers significantly more space for mutations that may remove the LxCxE motif without affecting sT-Ag. In order to test whether the absence of such mutations in MCC-derived tLT-Ags is statistically significant, we extracted from the NCBI database all unique tLT-Ag entries ($n = 40$) and identified the position of the last preserved amino acid, i.e., the last amino acid position preceding stop codon or frameshift mutations. As shown in Fig. 1A, most mutations ($n = 31$; 78%) result in truncation between aa 243 and 329 and remove the origin binding domain (OBD), whereas only 7 mutations (18%) leave the OBD intact. Furthermore, the 31 proximal mutations map upstream of the 57-kDa splice donor, such that the spliced transcripts would likewise generate a truncated LT-Ag. In 9 cases, the mutations are located within the 57-kDa intron, and these isolates should thus be able to produce a full-length 57-kDa T-Ag.

For each amino acid position encoded by the second exon of the full-length LT-Ag gene, we next calculated the *P* value for the hypothesis that this position is subject to either positive or negative selection in MCC (see Materials and Methods for details of the statistical analysis). The *P* values for negative selection of the LT-Ag carboxy terminus were highly significant, with the lowest *P* value observed for truncation after amino acid position 329 (*P* value, 1.76e-18) (Fig. 1A). In addition, our analysis strongly suggests positive selection for the first 165 aa encoded by the second exon, which includes the LxCxE motif (*P* value, 7.83e-10). In contrast, we found no evidence to suggest positive selection of the recently identified (50) functional nuclear localization signal (NLS) sequence located between aa 277 to 280 (*P* value, 0.13) or the sequences that are homologous to the NLS of SV40 LT-Ag (aa 299 to 307; *P* value, 0.60). Hence, the presence of these signals is not a general requirement for tLT-Ag functions during MCC pathogenesis.

MCC-derived truncated LT-Ags differ from full-length LT-Ags with regard to subcellular localization and steady-state expression levels. Given that a significant number of tLT-Ags (16 of 40; 38%) lack previously identified NLSs, we sought to investigate the expression and subcellular localization of representative LT-Ag truncation products. We therefore generated eukaryotic expression constructs for the full-length MCPyV LT antigen derived from a consensus MCPyV genome (28) as well as three truncated tLT-Ag genes isolated from MCC-derived cell lines (MCCL-12, -11, and -3) (18) and a shortened LT-Ag from the primary tumor MCC350 (3). As indicated in Fig. 1B, MCCL-11 is truncated 27 aa downstream of the LxCxE motif and represents the shortest LT-Ag isolate identified to date, whereas MCC350, MCCL-12, and MCCL-3 terminate 14, 32, and 49 aa further downstream, respectively. Of the four truncated LT-Ags, only MCCL-3 retains the functional NLS identified by Nakamura et al. (50). To ensure functionality of the N-terminally tagged full-length proteins, we performed viral DNA replication assays in the presence of an additional plasmid containing the minimal MCPyV origin of replication (39). As shown in Fig. 2, MCPyV-LT N-terminally fused to a FLAG tag or CFP is highly expressed and able to support DNA replication. This observation is in line with other studies reporting functionality of N-terminally tagged MCPyV LT proteins in replication assays, coimmunoprecipitation studies, and helicase assays (21, 29, 39). We used confocal microscopy in combination with the monoclonal antibody Cm2B4 (which recognizes aa 116 to 129 of LT-Ag) (9) to detect MCPyV LT in transfected H1299 cells. As shown in Fig. 3, full-length MCPyV LT-Ag (and SV40 LT-Ag, which was employed as a positive control) localized strictly to the nucleus. In contrast, all three MCC-derived LT-Ags that lack the NLS motif were distributed diffusely in the nucleus and the cytoplasm (Fig. 3). Interestingly, a substantial fraction of the MCCL-3-derived tLT-Ag (tLT-

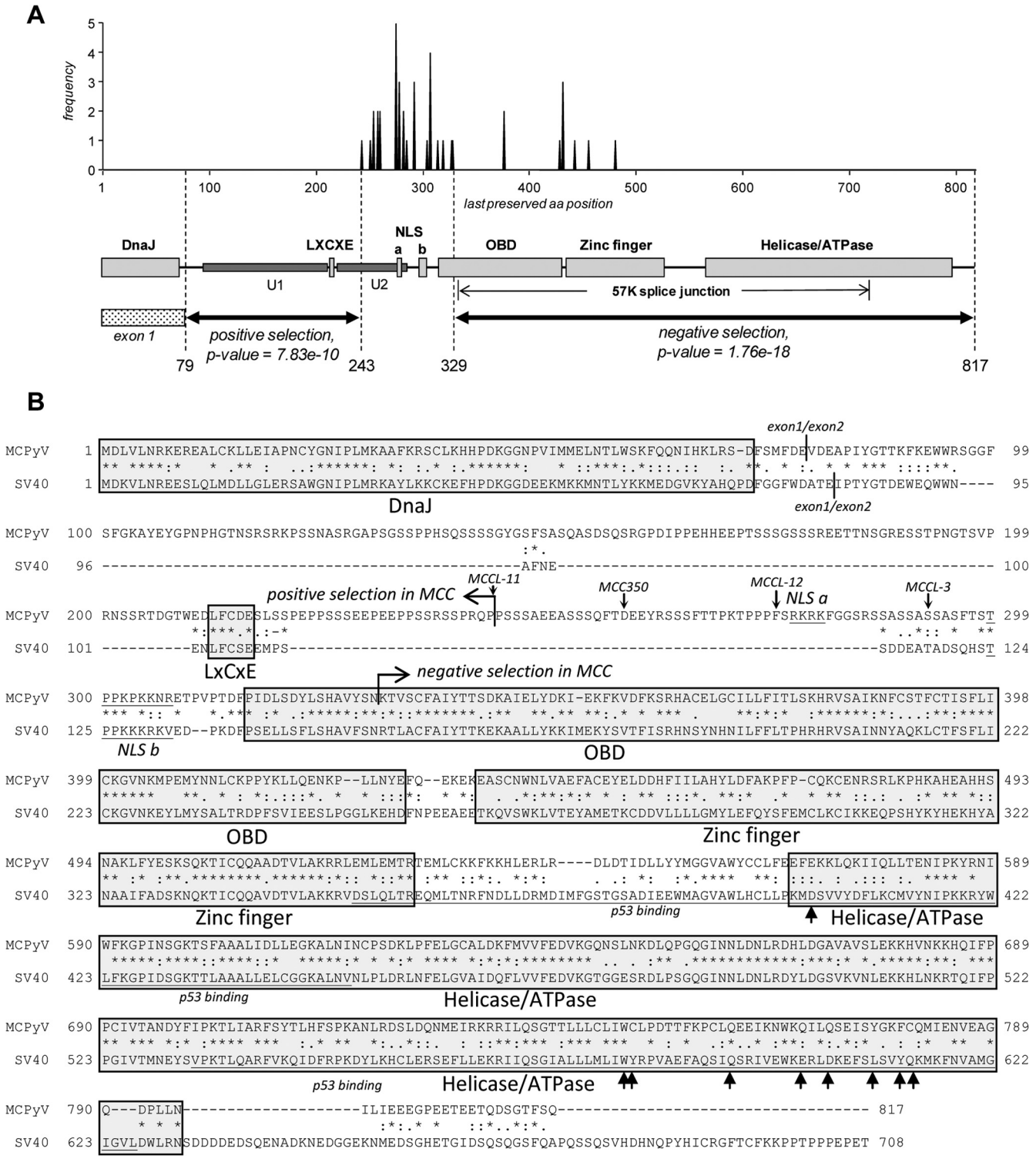

FIG 1 Preservation of the LxCxE motif in MCC-derived LT-Ag proteins is highly significant. (A) Frequency plot showing the position of the last preserved amino acid (i.e., the last position preceding stop codon or frameshift mutations) across 42 MCC-derived truncated MCPyV LT-Ag genes. (B) Amino acid alignment of SV40 LT-Ag (GI: 297591903) and MCPyV LT-Ag (GI: 372100550) using LALIGN. Identical, conserved, and semiconserved amino acids are indicated by asterisks, colons, and periods, respectively. The functional DnaJ, OBD, zinc finger, and helicase/ATPase domains, as well as the Rb binding LxCxE motif, are shown as light gray boxes in panels A and B. Regions that undergo positive or negative selection according to our statistical analysis are marked. In panel A, dark gray boxes labeled U1 and U2 symbolize regions that are unique to MCPyV and not present in SV40. The position of a recently identified functional NLS in MCPyV LT-Ag (50) and the partially conserved NLS of SV40 are labeled NLS a and b, respectively. Underlined amino acids in panel B highlight the bipartite regions that mediate p53 binding of SV40 LT-Ag, and individual residues that make direct contact with p53 are additionally marked by arrows (72).

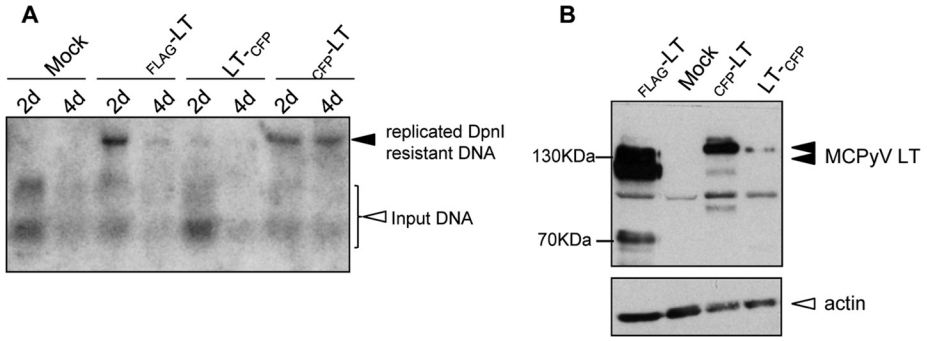

FIG 2 Viral replication assays using pCR2.1-ori plasmids and LT expression plasmids. (A) Southern blot of HIRT DNA extracts from PFSK-1 cells transfected with 1 μg pCR2.1 MCPyV-ori and N-terminally or C-terminally tagged MCPyV LT expression constructs. (B) Western blot of PFSK-1 cells expressing MCPyV LT-Ag 48 h posttransfection. Mock, mock transfection; d, days.

Ag_{MCCL-3}) likewise localized to the cytoplasm, even though this isolate retains an NLS and shows increased nuclear accumulation compared to the other tLT-Ags (Fig. 3). All tested proteins showed marked exclusion of nucleolar staining. To further corroborate these findings, we performed cell fractionation experiments with Merkel cell cancer cell lines as well as PFSK-1 cells transiently overexpressing MCPyV LT full-length and truncated protein (Fig. 4). In accord with our immunofluorescence data, the predominant fraction of MCC-derived truncated LT proteins can be detected in the cytoplasm. In WaGa cells, the truncated protein localizes almost exclusively to the cytoplasmic fraction, whereas in MKL-1 cells, the protein is present in the nuclear and cytoplasmic fractions (Fig. 4A). Similar results were obtained for cells with an ectopically expressed MCCL-11-derived tLT-Ag (Fig. 4B, upper panel). In contrast, full-length MCPyV LT-Ag was detected exclusively in the chromatin-associated nuclear fraction and the insoluble matrix (Fig. 4B, lower panel). We conclude from the above data that strict nuclear localization is not a general feature of MCC-derived shortened LT-Ags.

In our localization and Western blot studies, we repeatedly observed higher steady-state expression levels of truncated MCPyV LT-Ag than of the full-length protein (Fig. 3 and 4B and data not shown). Given these differences, the amounts of transfected expression constructs were titrated in subsequent experiments that required equal protein expression levels (Fig. 4) (discussed below). The reasons for the different expression efficiencies are currently unclear. Our constructs harbor the entire early region of MCPyV and thus should be principally able to express sT. Since the sT antigen was recently shown to positively influence LT stability (27), it would seem possible that the observed differences are due to preferential stabilization of truncated LT protein. However, we find this unlikely as we did not observe significant differences between the stability of ectopically expressed full-length and that of truncated LT proteins in half-life experiments (data not shown). We found the C-terminal coding region of the LT open reading frame (ORF) to be substantially enriched in rare codons (data not shown) and therefore suspect that translation efficiency may be a contributing factor. However, as we did not measure transcript abundance, it is also possible that there are differences on the transcriptional level.

Full-length MCPyV LT-Ag coprecipitates with p53 and inhibits p53-dependent transcription. The ability of SV40 LT-Ag to transform cells correlates with its ability to interact with the

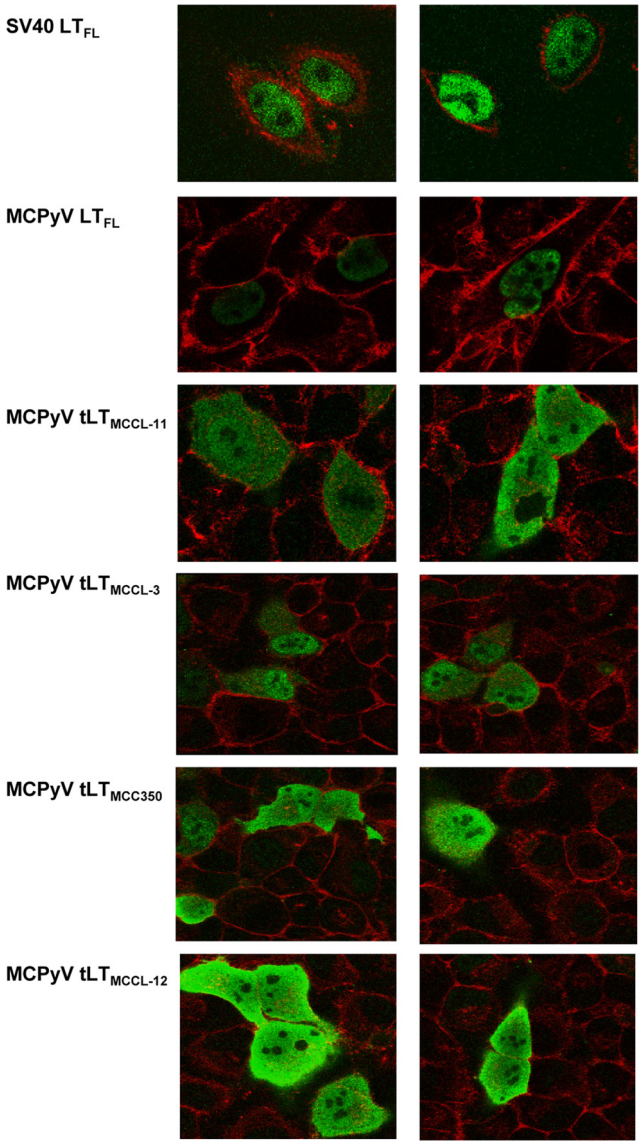

FIG 3 Subcellular localization of full-length SV40 LT_{FL}, full-length MCPyV FL, and truncated LT proteins (MCPyV tLT) overexpressed in H1299 cells. Confocal microscopy shows LT protein localization using Pab419 MAb and Cm2B4 MAb, fluorescein isothiocyanate (FITC)-conjugated secondary antibodies. F-actin was stained with Cy5 phalloidin. SV40 LT_{FL} localization stained with Pab419 was used as a control.

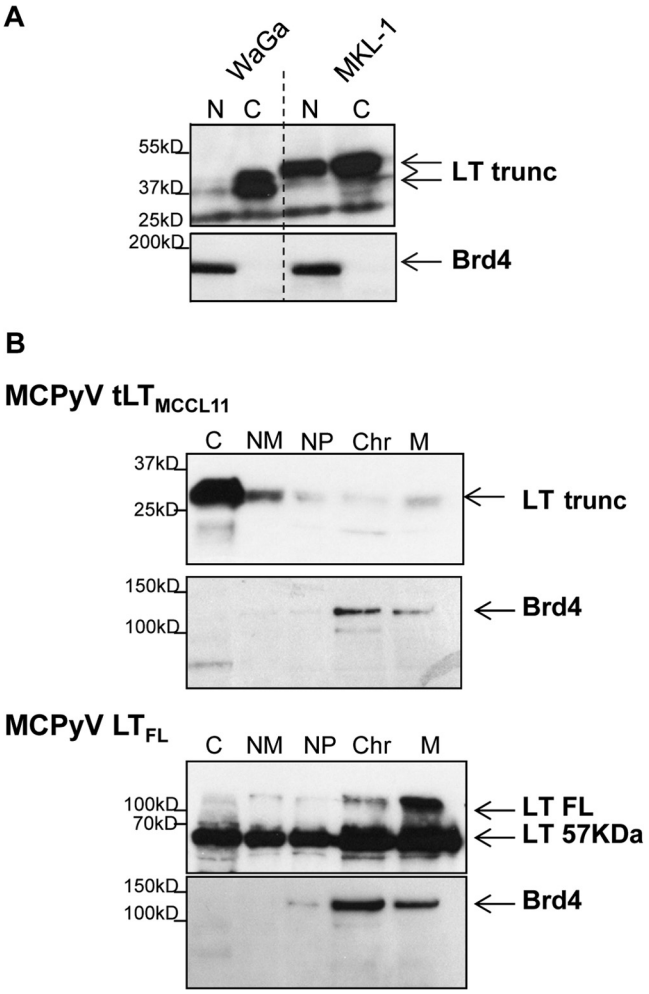

FIG 4 Cell fractionation of Merkel cell cancer (MCC) cell lines and PFSK-1 cells overexpressing MCPyV LT_{FL} or MCC-derived truncated MCPyV tLT. (A) MCPyV-positive MCC cell lines MKL-1 and WaGa and MCPyV-negative MCC cell line UISO were subjected to cell fractionation. Nuclear (N) and cytoplasmic (C) extracts were analyzed by Western blotting, applying MCPyV LT-specific Ab Cm2B4 and, as a control, a specific antibody recognizing the nuclear protein Brd4. (B) PFSK-1 cells transiently overexpressing full-length MCPyV LT_{FL} and truncated MCPyV $tLT_{MCCL-11}$ were analyzed by cell fractionation. Cell fractions corresponding to cytoplasm (C), nuclear matrix (NM), nucleoplasm (NP), chromatin (Chr), and insoluble matrix (M) were analyzed by Western blotting. trunc, truncated.

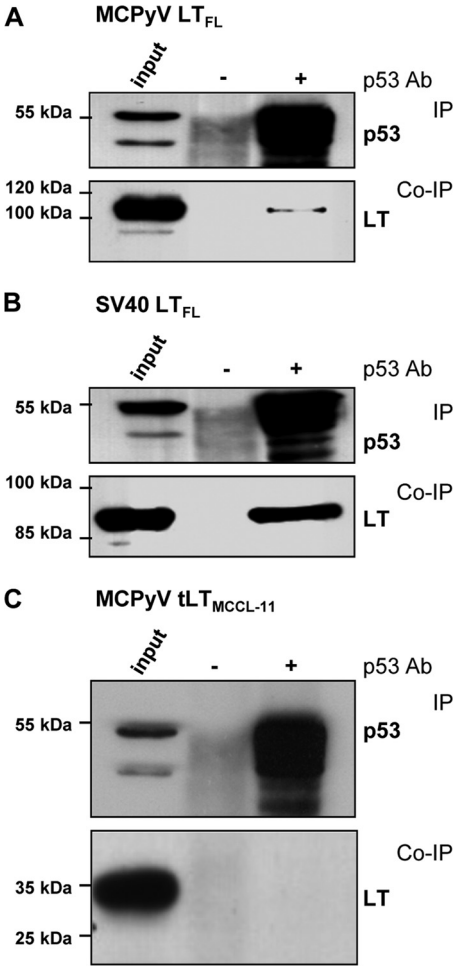

FIG 5 MCPyV LT_{FL} coprecipitates p53 in transiently transfected H1299 cells, while truncated MCPyV tLTs fail to interact with p53. Cells were cotransfected with p53 and different LT-Ag constructs encoding full-length MCPyV LT_{FL} (A), full-length SV40 LT_{FL} (B), or truncated MCPyV $tLT_{MCCL-11}$ (C). Upper blots represent immunoprecipitation of p53 using rabbit polyclonal α-p53 (FL-393) coupled to Sepharose. Lower blots represent coprecipitated proteins. Ten percent of the input and 50% of the co-IP complex are shown in the each lane.

tumor suppressor proteins Rb and p53 (14). As shown in Fig. 1B, the bipartite binding region of SV40 LT-Ag as well as individual amino acids that make contact with p53 are not well conserved in MCPyV. In order to directly investigate the ability of full-length MCPyV LT-Ag to bind to p53 or p53-containing complexes, we performed coimmunoprecipitation analyses of ectopically expressed p53 and MCPyV LT-Ag in 293 (data not shown) and H1299 (Fig. 5) cells. As shown in Fig. 5A and C, we observed that an antibody against p53 can indeed coprecipitate full-length MCPyV LT-Ag but not an MCC-specific truncated LT protein. The amount of coprecipitated full-length MCPyV LT protein, however, was considerably lower than that of SV40 LT-Ag (Fig. 5B).

To examine the consequences of LT-Ag binding on p53-mediated transactivation, p53-negative H1299 cells were cotransfected with expression constructs for wt p53 (pCN-53), LT-Ag, and the p53-dependent luciferase reporter construct pRE-luc. The reporter contains five artificial p53 binding sites, such that luciferase activity directly correlates with p53-dependent transcription activation. The adenoviral protein E1B55K-wt (51, 52) and SV40 LT-Ag were used as positive controls. Given the differences in expression efficiency as described above, in order to allow direct cross-comparison between the various LT-Ags we titrated the amount of transfected full-length and truncated MCPyV LT-Ag expression constructs such that at the highest concentration, the protein levels were approximately equal and comparable to those seen for SV40 LT-Ag (Fig. 6B). As shown in Fig. 6A, SV40 LT-Ag reduced p53-dependent transcription by 72%. Full-length MCPyV LT-Ag likewise inhibited p53-dependent transcription in a dose-dependent manner, although to a lesser degree (60% at the highest expression level). In accord with the results obtained in the coimmunoprecipitation experiments, the truncated MCPyV LT

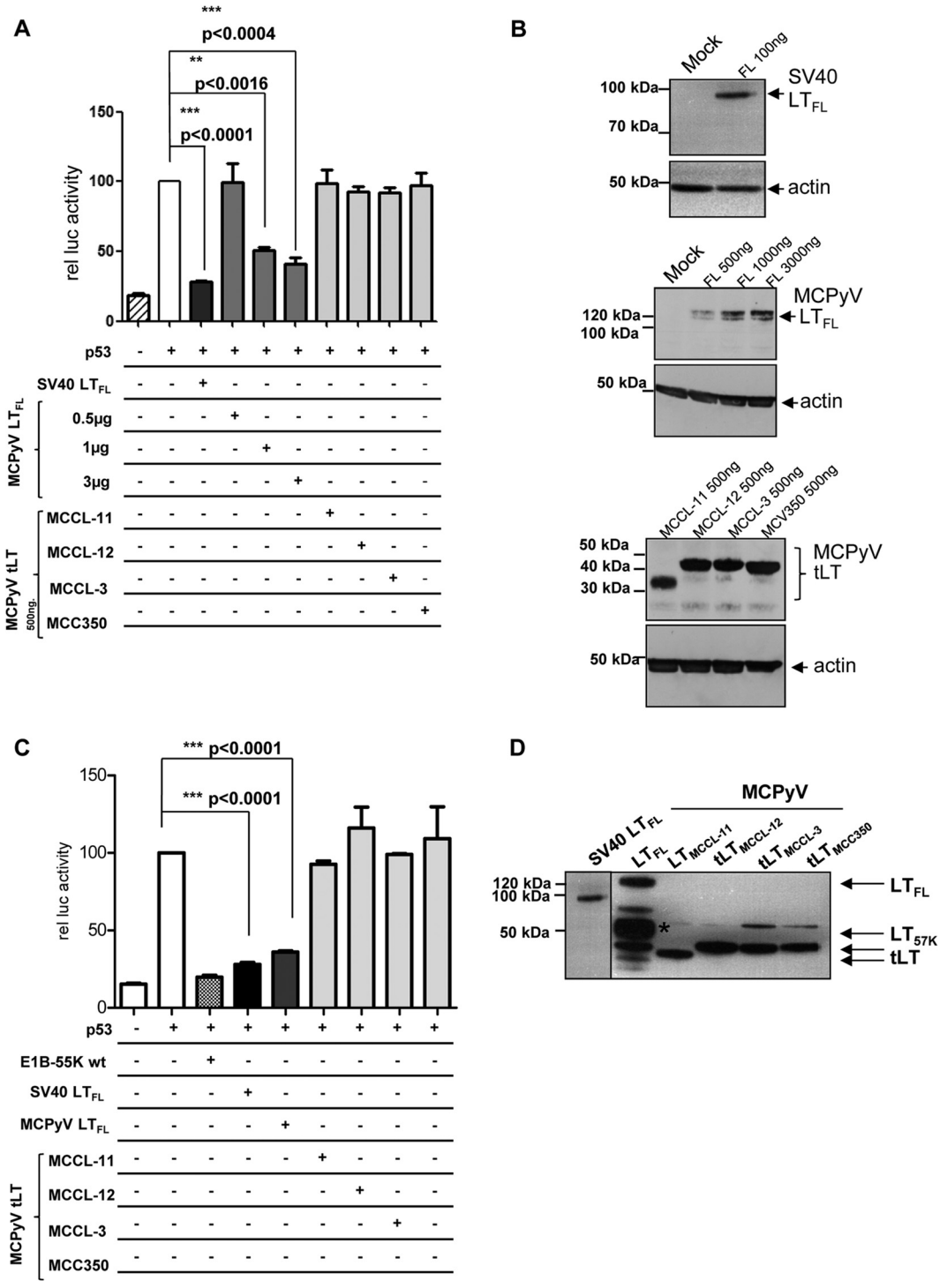

FIG 6 MCC-derived truncated MCPyV tLT proteins do not repress p53-dependent transcription in transiently transfected H1299 cells. Subconfluent H1299 cells were transfected with pRL-TK, pRE-Luc, pc53-SN3, and LT-Ag expression constructs (100 ng pZIPTEX-SV40LT$_{FL}$, 3 µg pCMV2b-MCPyVLT$_{FL}$, 200 ng pCMV2b-MCPyVLT$_{MCCL\text{-}12}$, 200 ng pCMV2b-MCPyVLT$_{MCCL\text{-}11}$, 200 ng pCMV2b-MCPyVLT$_{MCCL\text{-}3}$, 200 ng pCMV2b-MCPyVLT$_{MCV350}$). DNA amounts were adjusted with empty vector such that the total amount of transfected DNA was equal in each sample. The cells were harvested after 48 h and analyzed for firefly luciferase activity and *Renilla* luciferase activity. (A) Normalized luciferase activity relative to that of the positive control (cells transfected with p53 and reporter constructs) is shown. Adenovirus E1B-55k-wt protein efficiently repressing p53-dependent transcription was used as an internal control. *P* values using an unpaired *t* test are indicated. (B) Western blot of cells analyzed in panel A with loading of equal amounts of LT protein expressed under these conditions. Unspecific background binding of Cm2B4 Ab staining is indicated with an asterisk.

TABLE 1 FACS-FRET results

Construct		CFP/YFP distance[a]	FRET signal (%)[b]		
YFP	CFP		Expt A	Expt B	Expt C
SV40 LT N	p53 N	1	0.4	1.5	1.4
SV40 LT N	p53 C	1	0	0	0
SV40 LT C	p53 N	2	24.4	20.7	29.3
SV40 LT C	p53 C	3	76.4	80.1	71.1
p53 N	SV40 LT N	1	0.7	0.9	0.2
p53 C	SV40 LT N	1	1.6	1.9	0.4
p53 N	SV40 LT C	2	41.1	40.2	44.5
p53 C	SV40 LT C	3	47.3	32.1	36.2
MCPyV LT N	p53 N		0	0	0
MCPyV LT N	p53 C		0	0	0
MCPyV LT C	p53 N		0	0	0
MCPyV LT C	p53 N		0	0	0
p53 N	MCPyV LT N		0	0	0
p53 C	MCPyV LT N		0	0	0
p53 N	MCPyV LT C		0	0	0
p53 C	MCPyV LT C		0	0	0
MCPyV tLT N	p53 N		0	0	0
MCPyV tLT N	p53 C		0	0	0
MCPyV tLT C	p53 N		0	0	0
MCPyV tLT C	p53 C		0	0	0
p53 N	MCPyV tLT N		0	0	0
p53 N	MCPyV tLT C		0	0	0
p53 C	MCPyV tLT N		0	0	0
p53C	MCPyV tLT C		0	0	0

[a] Calculated distance of FRET partners using PyMOL. 1, distance of 7 to 14 nm, nonparallel; 2, distance of 8 to 14 nm, parallel; 3, distance of 4 to 7 nm, parallel.
[b] Three independent measurements (shown here as experiments A, B, and C) were taken.

proteins did not significantly influence transactivation of the reporter construct by p53.

Full-length MCPyV LT-Ag does not directly bind to p53. LT-Ag proteins encoded by SV40, BK virus, and JC virus have been shown to directly bind to p53 (15, 53–58), whereas mouse polyomavirus LT-Ag does not bind p53 or inhibit p53-dependent transcription (59). To investigate whether the observed coprecipitation of MCPyV LT antigen with p53 is due to direct or indirect binding, we performed FACS-FRET experiments with living cells, as recently described (44), using different cell lines that ectopically express MCPyV LT or SV40 LT proteins and p53 as YFP or CFP fusion proteins. FRET is based upon the transfer of energy from an excited donor fluorophore to a close-by acceptor fluorophore. As this transfer occurs only when the distance between donor and acceptor is below 8 nm, indirect interactions are much less likely to yield a positive signal than are direct interactions. All proteins were N- and C-terminally tagged in all possible combinations in order to minimize the risk of producing false-negative results that may be the consequence of tag-induced structural alterations. Confocal microscopy was performed for all p53 and LT-Ag constructs to confirm expression and proper subcellular localization patterns (data not shown). Although N-terminally fused SV40 LT-Ags proved nonfunctional (potentially due to structural disturbances of the fusion product), cotransfection of all C-terminally fused SV40 LT-Ags and p53 resulted in highly significant FACS-FRET signals, with an average of 45% for different cell lines (293, H1299, and PFSK-1 cells), thus readily confirming the direct interaction between the two proteins *in vivo* (Table 1). In contrast, we did not measure any FRET signal for N- or C-terminally tagged MCPyV LT fusion proteins (full-length or truncated) (Table 1 and data not shown) or for any of the various p53 fusions, indicating that MCPyV LT-Ag most likely does not directly bind to p53.

MCPyV FL and truncated LT-Ag bind to Rb and release Rb-dependent repression of E2F-regulated transcription. The ability of tumor-derived truncated full-length and LT proteins of MCPyV to bind to Rb through the highly conserved LxCxE motif has previously been confirmed by coimmunoprecipitation experiments (9). Here, we compared coprecipitation efficiencies of Rb and SV40 LT-Ag as well as full-length and truncated MCPyV LT proteins. As in our previous p53 binding studies, we used a larger amount of the full-length MCPyV expression construct to obtain expression levels comparable to those of the truncated proteins. As shown in Fig. 7A and B, the full-length MCPyV LT protein bound weakly to Rb in transiently transfected H1299 cells compared to results with SV40 LT-Ag. Interestingly, as shown in Fig. 7, a considerably more substantial fraction of the truncated MCCL-11 protein was coprecipitated by the Rb antibody (compare the amount of coprecipitated LT-Ag to the input in the lower panels of Fig. 7A and C). Likewise, experiments using a FLAG antibody to pull down LT-Ag revealed that all MCC-derived LT-Ag proteins coprecipitated substantially larger amounts of Rb protein than full-length protein (Fig. 7D to F). We obtained similar results with PFSK-1 cells (data not shown), suggesting that more efficient binding to Rb is a general feature of truncated LT proteins.

We next investigated functional consequences of the interaction between MCPyV LT-Ag proteins and Rb by measuring the release of Rb-dependent transcriptional repression (Fig. 8). For this purpose, we performed transcriptional derepression assays using Rb-negative Saos-2 cells transfected with a luciferase reporter construct containing the E2F-dependent H2A promoter (35), expression constructs for Rb and E2F, and either an empty vector control or expression constructs for LT proteins. SV40 LT-Ag, for which release of Rb from E2F has been described before (14, 60), was used as a positive control. As shown in Fig. 8, coexpression of Rb and E2F in Saos-2 cells resulted in repression of luciferase expression to approximately 30% of the levels seen after transfection of the E2F construct alone. Simultaneous expression of SV40 LT-Ag resulted in a partial rescue of Rb-mediated transcriptional repression to 50% of baseline levels. Coexpression of full-length MCPyV LT, as well as truncated MCPyV LT proteins (comparable protein expression levels were applied), likewise relieved repression by Rb, restoring luciferase expression to 55 to 65% of that of the E2F-only control. Although derepression was slightly more efficient for the truncated LT proteins, the differences between the individual MCPyV LT proteins were not statistically significant (*P* value, 0.0647; 95% confidence interval) in this assay.

To further follow up on these results, we performed real-time RT-PCR experiments with PFSK-1 cells transiently transfected with the MCPyV LT expression constructs indicated in Fig. 9. Similar to previous experiments, transfected DNA amounts were adjusted to ensure equal LT protein expression levels (Fig. 9B). At 48 h posttransfection, quantitative RT-PCR was performed to quantify expression levels of the cdc2 and cyclinA2 E2F target genes. Quantification of GAPDH and RPL13 levels was used for normalization purposes. As shown in Fig. 9A, we find a significant

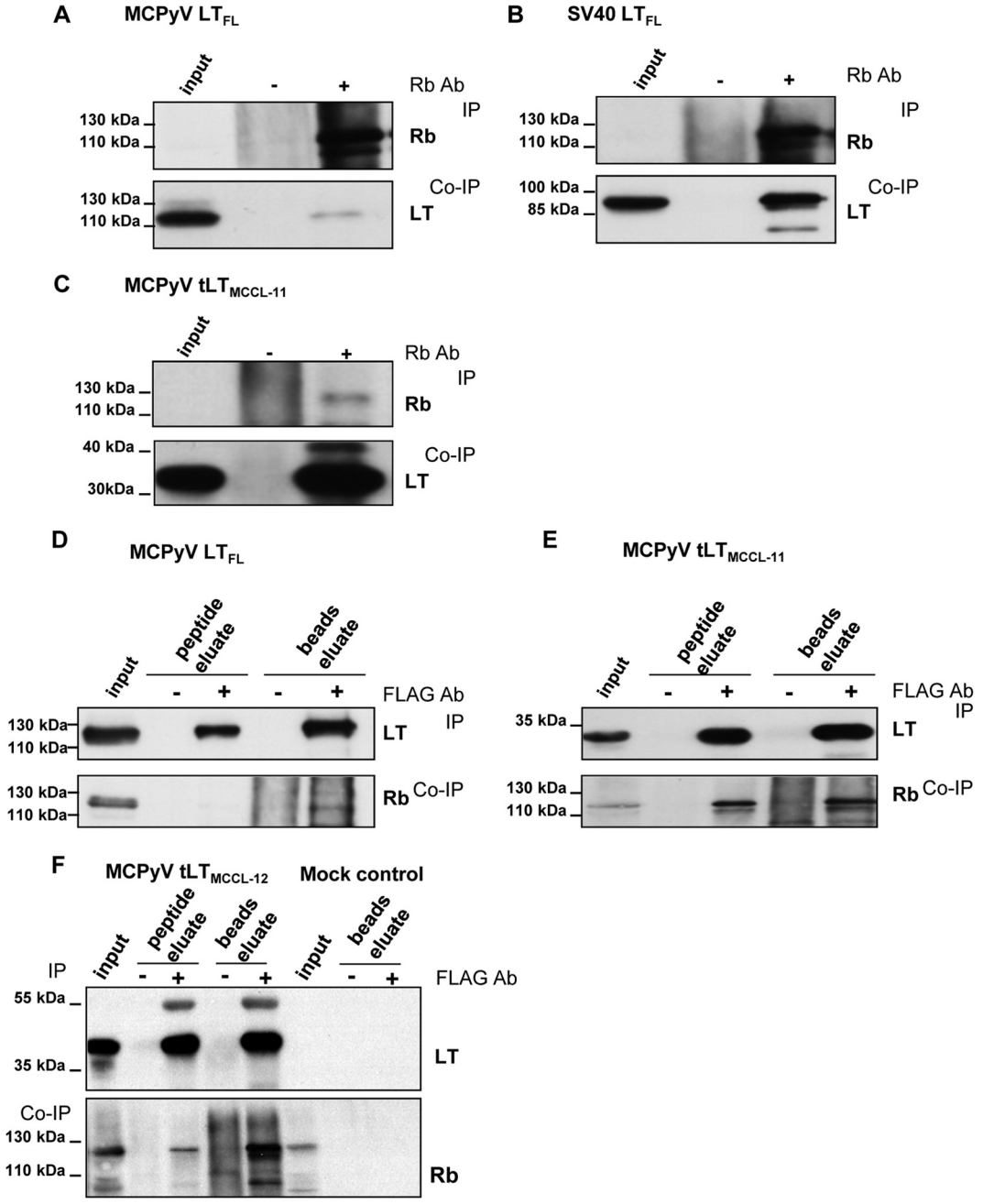

FIG 7 Full-length MCPyV LT$_{FL}$ weakly binds Rb in transiently transfected H1299 cells while truncated MCPyV tLT strongly interacts with Rb. Cells were cotransfected with Rb and LT expression constructs. To ensure equal levels of expression, 3 μg of the full-length LT and 0.5 μg of truncated LT expression constructs were used. Empty vector was used to the total amount of transfected DNA such that it was equal in each sample. Cells were harvested after 72 h, and total-cell extracts were prepared. Coimmunoprecipitation of MCPyV LT$_{FL}$ (A), SV40 LT$_{FL}$ (B), and MCPyV tLT (C) using polyclonal Rb serum for precipitation of interacting proteins. (D) Full-length MCPyV LT FL or truncated MCPyV tLT proteins (E and F) were precipitated with an anti-FLAG antibody; coprecipitating proteins were eluted with FLAG peptide (peptide eluate). In addition, beads were boiled in sample buffer (beads eluate). Cell lysate from H1299 cells transfected with a vector control (Mock control) were used as a negative control in co-IP experiments. Beads were boiled in sample buffer to control for unspecific binding.

increase in cdc2 and cyclinA2 expression when truncated MCPyV LT protein or SV40 LT protein was expressed. In contrast, MCPyV LT full-length protein expression did not induce a significant increase of cdc2 and cyclinA2 expression levels. These data suggest that, at least under the conditions used here, truncated LT is more potent than the full-length protein in its ability to induce transcription of authentic E2F target genes.

Truncated MCPyV LT-Ag display high binding affinity to the Rb pocket domain. To follow up on our coimmunoprecipitation results, where we consistently observed robust binding of Rb to truncated MCPyV-LT proteins, we sought to further investigate parameters of the interaction by use of microscale thermophoresis (MST), a novel method that allows the quantitative measurement of binding affinities between proteins in solution (61). For this

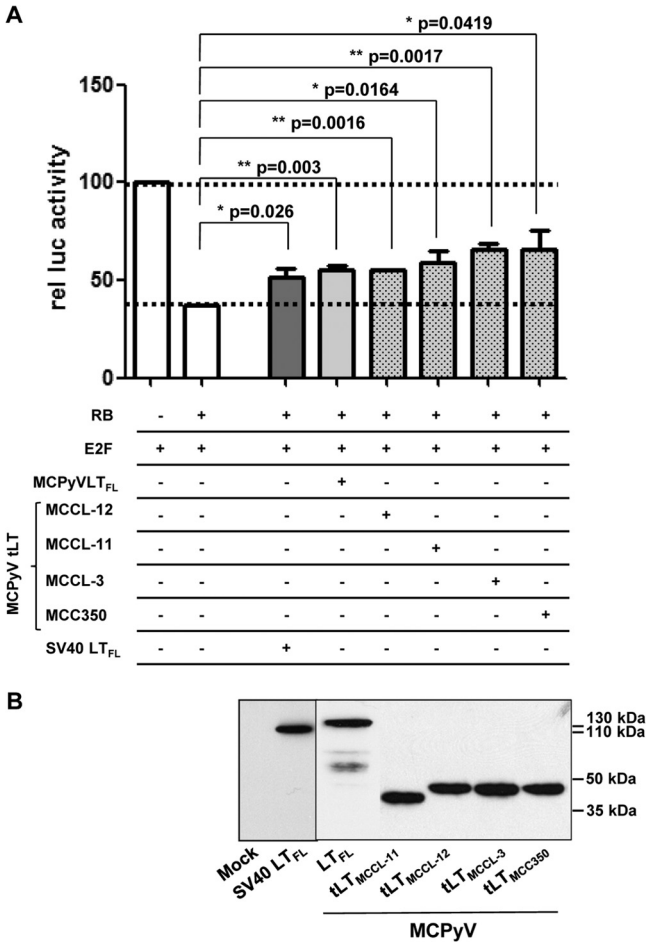

FIG 8 Release of Rb-dependent repression by tumor-derived truncated MCPyV tLT. (A) Reporter construct pI-H2A-68 was cotransfected with an Rb expression plasmid in the presence of E2F and the indicated LT proteins into Saos-2 cells. Luciferase activity (rel luc activity; firefly and *Renilla* luciferase to normalize for transfection differences) was determined 48 h after transfection. E2F-induced transcription activity was set to 100, and release of repression by LT-Ag is indicated. (B) Equal levels of LT-Ag expression were confirmed by Western blotting.

purpose, we bacterially expressed a His-tagged MCPyV LT-Ag fragment corresponding to the MCCL-11 isolate (MCPyV LT_{1-244}) as well as a His-tagged amino-terminal fragment of SV40 LT-Ag spanning amino acids 7 to 117 (a region that had been previously used in cocrystallization studies of SV40 LT-Ag and the Rb pocket domain [62]) and purified both proteins by Ni-NTA and size exclusion chromatography. The pocket domain of Rb was expressed as a GST fusion protein (GST-$Rb_{382-771}$) and likewise purified by affinity chromatography, followed by thrombin cleavage and ion-exchange chromatography. The purified Rb protein was fluorescently labeled and kept at a constant concentration of 33 nM, whereas the MCPyV and SV40 LT proteins were titrated over a range of 0.13 to 531 and 0.82 to 6725 nM, respectively. As shown in Fig. 10, at a salt concentration of 150 mM NaCl, we observed an average binding affinity of 1950 nM between SV40 LT and the Rb pocket domain. Interestingly, at the same salt concentration, MCPyV tLT-Ag exhibited a significantly higher binding affinity of 51.3 nM. At an elevated salt concentration of 250 mM, MCPyV still bound to Rb with an average affinity of 121 nM (Table 2), whereas no binding could be observed for SV40 LT-Ag under these conditions.

Rb mislocalizes to the cytoplasm in cells expressing truncated MCPyV LT protein. Considering the high-affinity between MCPyV tLT-Ag and Rb and the fact that a substantial fraction of NLS-containing and NLS-deficient MCPyV LT proteins localize to the cytoplasm, we next investigated the subcellular localization of Rb in LT-Ag-expressing cells. For this purpose, H1299 cells were transiently transfected with Rb and SV40 or full-length or truncated MCPyV LT-Ag expression constructs. At 48 h post-transfection, cells were analyzed by double staining and confocal laser scanning microscopy. As shown in Fig. 11, Rb exhibited the expected nuclear localization in cells that express full-length SV40 or MCPyV LT protein. In contrast, upon expression of tumor-derived truncated MCPyV LT-Ag, a significant portion of Rb shows redistribution to the cytoplasm, where it colocalizes with shortened LT-Ag. Endogenous Rb protein shows a very similar behavior in cells that ectopically express truncated MCPyV LT protein (data not shown).

MCC-derived T-Ag region induces cell transformation. Expression of SV40 LT-Ags can transform primary rodent fibroblasts, resulting in focus formation and multilayered cell growth of the transformed cells, whereas untransformed cells undergo senescence and cell death after a few weeks. Human polyomavirus BK- or JC-derived LT-Ag also transforms primary rodent fibroblasts, albeit with lower efficiency (63). Shuda and colleagues demonstrated that MCPyV sT-Ag, but not MCPyV LT-Ag, induces focus formation in low-passage-number immortalized rat-1 fibroblasts (25). Recent publications using already immortalized rodent cells transfected with LT-Ag-expressing plasmids showed that truncated MCPyV LT proteins support cell growth of these cells under low-serum conditions and in anchorage-independent growth assays (21, 29). However, transformation of primary rodent cells by MCPyV T-Ags has not been described to date. We compared the transforming potential of SV40 LT-Ag and full-length or shortened MCPyV T-Ag proteins expressed in the context of the complete MCPyV early region (these constructs are thus principally able to express sT as well as LT). Figure 12A shows a representative result of quantitative focus formation assays in primary baby rat kidney (pBRK) cells. The transiently transfected SV40 and MCPyV T proteins induced substantial focus formation in pBRK cells, leading to the outgrowth of multilayered aggregates of pBRK cells within 28 days. Interestingly, the constructs encoding tumor-derived truncated LT-Ag genes yielded similar or higher transforming potential than that of the wt gene, although they were unable to interfere with p53-dependent transcription, with the exception of one isolate (MCCL-12). Individual colonies could be isolated from all transformed cell cultures (including MCCL-12) and continued to express MCPyV LT-Ag upon subculturing, although at lower levels than those for SV40 LT-Ag-transformed cells (Fig. 12B). However, in contrast to the truncated protein, isolated pBRK colonies expressing the full-length MCPyV LT protein could not be passaged more than 3 or 4 times. As shown by the example of MCCL-3-derived LT-Ags in Fig. 12C, we also observed that cells transformed by MCPyV T-Ags are capable of anchorage-independent growth in soft agar, yet they generally form smaller colonies and grow significantly slower than their SV40-transformed counterparts. These results were confirmed by an anchorage-independent growth assay using low-passage-number NIH 3T3 cells expressing LT proteins (Fig. 12D).

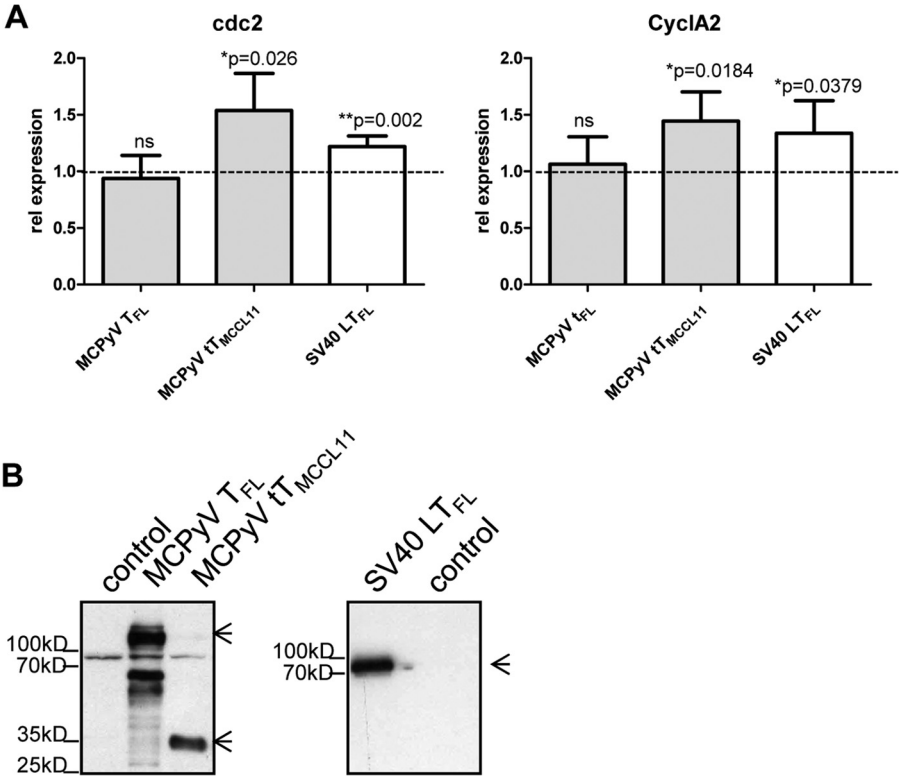

FIG 9 Transcription of E2F-dependent genes cdc2 and cyclin A2 is upregulated in cells overexpressing truncated MCPyV tLT-Ag. PFSK-1 cells were transiently transfected with the indicated LT expression plasmids or a control plasmid. At 48 h posttransfection, total RNA was isolated and real-time RT-PCR was performed (A). Values were normalized against two housekeeping genes, and values for the control plasmid were set to 1. Values represent the averages from four independent experiments, with error bars indicating the standard deviations. *P* values indicate a significant difference from results for the vector control. (B) Western blot of the transiently transfected cells used in panel A. Arrows indicate full-length LT-Ag or truncated LT-Ag.

In summary, we show for the first time that tumor-derived MCPyV T-Ag genes are oncogenes that induce substantial alterations in morphology and growth behavior of primary rodent epithelial cells, despite the inability of tLT-Ags to bind to p53 or reduce p53-dependent transcription.

DISCUSSION

In this study, we performed a biochemical, molecular, and functional characterization of full-length and MCC-derived truncated MCPyV LT proteins. Key findings of our study include the facts that (i) truncated LT-Ags bind with high affinity to Rb and release transcriptional repression, (ii) full-length, but not truncated, MCPyV LT-Ag binds indirectly to p53 and interferes with p53-dependent transcriptional activation, and (iii) full-length and MCC-derived T-Ag genes can induce the transformation of primary rat epithelial cells.

MCPyV is the only human polyomavirus known to induce tumors in its host. A number of findings suggest a causative role of MCPyV in Merkel cell carcinoma tumorigenesis: the virus can be identified in the majority of MCC biopsy specimens (3, 4, 6–9), MCPyV DNA is monoclonally integrated in the tumor cells (3, 9), the viral T-Ags are expressed in tumor cells (5, 10), and LT-Ag sequences isolated from tumor cells harbor tumor-specific muta-

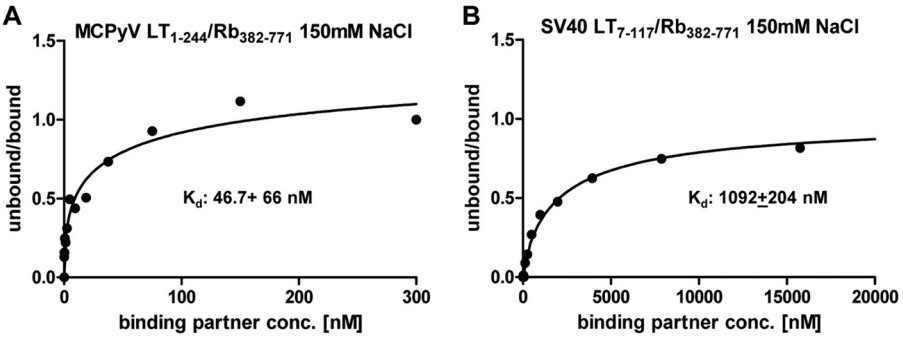

FIG 10 Binding affinity of truncated LT proteins to Rb pocket domain determined by microscale thermophoresis. Binding curves of bacterially expressed and purified His-tagged MCPyV LT_{1-244} (A) or SV40 LT_{7-117} (B) binding to the Rb pocket domain $Rb_{382-771}$ at a 150 mM salt concentration (conc.). Fitting curve and parameters are depicted.

TABLE 2 K_d values determined by microscale thermophoresis[a]

Construct	K_d value for $Rb_{382–771}$	
	150 mM NaCl	250 mM NaCl
SV40 LT_{7-117}	1950 nM (367.5)	—
MCPyV LT-Ag_{1-244}	51.3 nM (38.1)	121 nM (35.2)

[a] Average K_d value of three independent measurements by applying microscale thermophoresis. Standard deviations are indicated in parentheses. —, no binding.

tions that lead to premature truncation of LT-Ag, presumably due to a selection pressure to abrogate viral replication (9, 18, 64, 65). It is striking that all truncated LT proteins retain the LxCxE motif, a fact that would seem to provide a strong argument for a dominant requirement for LT-Ag-mediated Rb inactivation during MCC pathogenesis. Support for this hypothesis comes from the observation that knockdown of pan-T-Ag expression in sT- and LT-positive MCC cell lines results in growth arrest and subsequent cell death and is qualitatively different from a knockdown of sT-Ag only (26). Interestingly, however, Shuda and colleagues recently demonstrated that approximately 5 to 10% of MCCs express sT antigen but are negative for LT protein expression (25). Since sT-Ag, but not LT-Ag, was also found to be able to transform rat-1 cells (25), it could be argued that sT-Ag may represent the major oncogene of MCPyV. In such a scenario, it also appears possible that preservation of the LxCxE motif in LT-Ag is an indirect result of the pressure to maintain a functional sT-Ag gene. Our survey and a statistical analysis of truncated LT-Ag coding regions, however, clearly indicate that MCC development selects for the presence of an amino-terminal region that significantly extends beyond the first exon shared with the sT-Ag gene and which includes the LxCxE motif. As this selection also applies to the integrated genomes of those MCC tumors that have ceased to express LT-Ag (25), it appears likely that unequivocal expression of truncated, LxCxE-containing LT proteins is of critical impor-

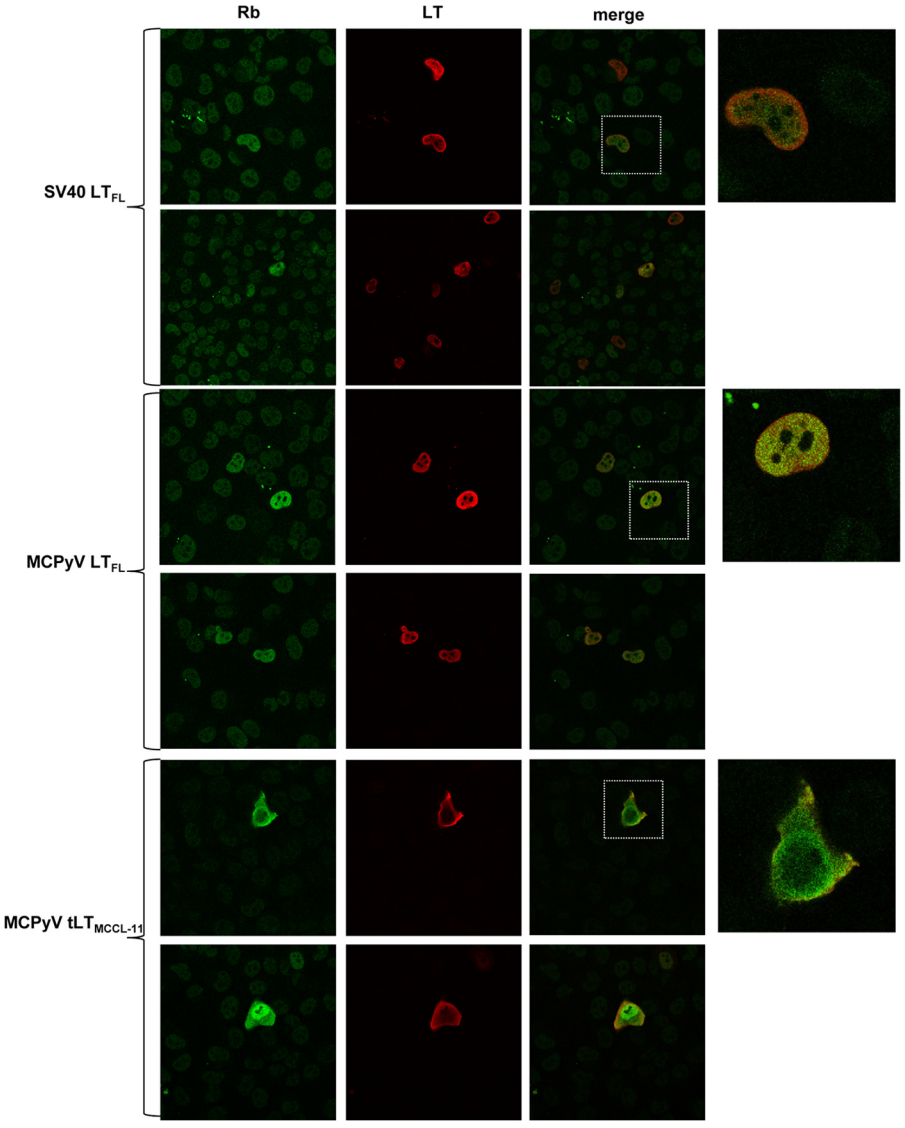

FIG 11 Subcellular localization of Rb protein in cells transiently transfected with truncated MCPyV tLT-Ag. H1299 cells were transiently transfected with Rb and the indicated LT expression plasmids. At 48 h posttransfection, cells were stained with Cm2B4 MAb, Pab419 MAb, and FITC (Rb)/TRITC (LT)-conjugated secondary antibodies.

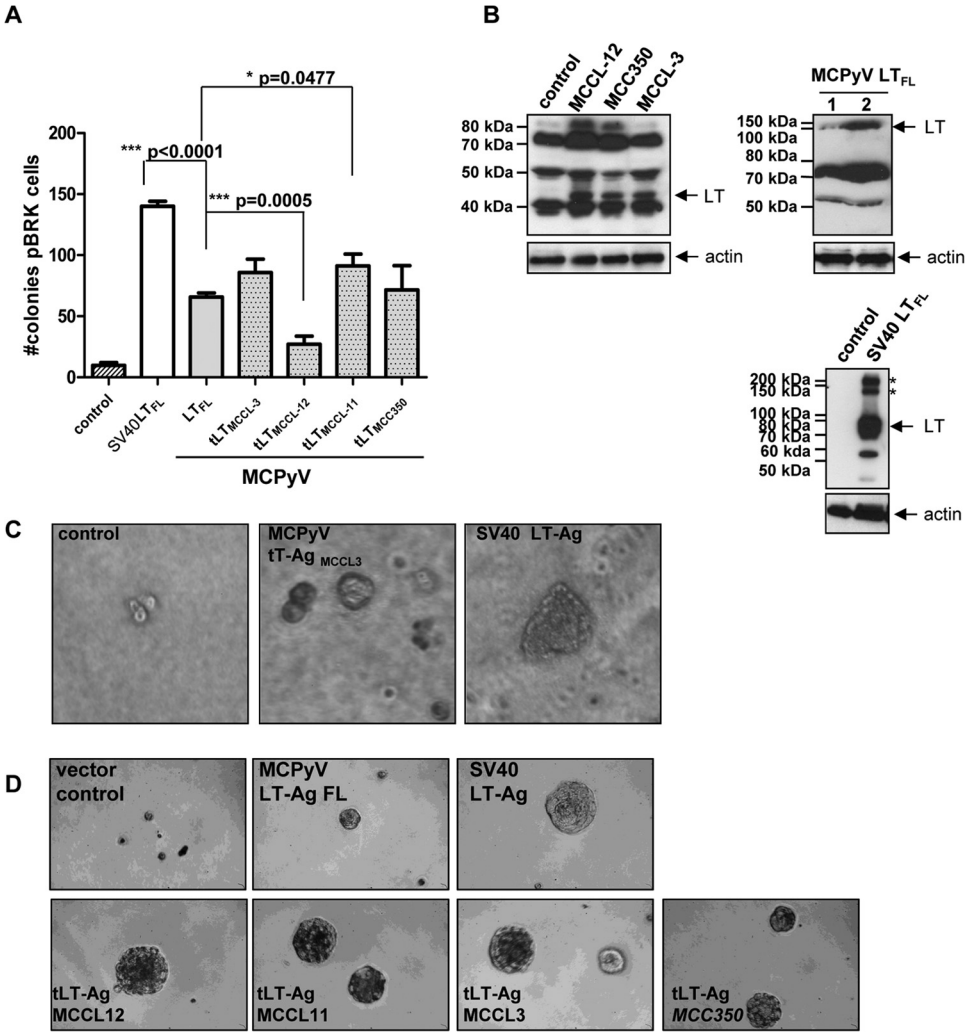

FIG 12 Transformation of primary baby rat kidney (pBRK) cells. (A) pBRK cells were transiently transfected with pCMV2 plasmids expressing full-length MCPyV LT_{FL}-Ag, truncated MCPyV tLT-Ag protein, or SV40 LT_{FL}-Ag. Colonies were quantified 28 days posttransfection. *P* values using an unpaired test are indicated. The experiment was performed six times in duplicate. (B) Western blot analysis of individual cell clones isolated in panel A. Thirty-five micrograms of total protein extract was loaded for MCPyV LT-expressing pBRK cells, while for SV40 LT expressing cells, only 10 μg total protein was loaded. LT-Ag proteins are highlighted with an arrow; the asterisk indicates the position of SV40 LT multimers. (C and D) Anchorage-independent growth of pBRK cell lines transformed with SV40 LT_{FL} or truncated MCPyV tLT-MCCL-3 (C) and NIH 3T3 cells stably expressing LT proteins (D); individual pictures were taken with phase contrast (×20) 28 days past seeding.

tance especially during the early steps of MCC tumorigenesis. At later stages, a subset of MCC tumors may become independent of continuous LT-Ag expression, perhaps as a result of the acquisition of additional mutations within the cellular genome and immunological pressure to limit viral gene expression. Recent publications by Cheng et al. and Li et al. demonstrated by using immortalized cells that truncated MCPyV-LT proteins, in contrast to full-length LT protein, efficiently promote cell growth (21, 29); this result suggests that the MCC-specific truncations of LT-Ag may serve to abrogate growth inhibitory properties mapping to the C terminus of MCPyV LT protein.

In contrast to the preserved LxCxE motif, our analysis suggests that there is no positive selection for the presence of a functional NLS in MCC-derived tLT-Ags. At a calculated molecular mass of 30.5 kDa or less, truncated LT proteins that lack an NLS should nevertheless be able to enter the nucleus via passive diffusion, a hypothesis that is supported by our localization studies. Interestingly, besides the nuclear LT-Ag fraction, we find that a considerable subfraction of not only NLS-deficient but also truncated LT-Ags that still contain an NLS localizes to the cytoplasm. Given the fact that similar observations were made for the MCC-derived cell line MKL-1 (which likewise expresses a tLT that still contains the reported NLS), one might argues against the possibility that the partial cytoplasmic localization occurs only during ectopic expression. This observation raises the possibility that an additional feature of truncated LT-Ags may be their ability to relocalize interaction partners to the cytoplasm. We have shown through examples that this is the case for ectopically and endogenously expressed Rb protein. Of note, we think it unlikely that the partial cytoplasmic relocalization of Rb itself has functional consequences, given that full-length (and strictly nuclear) LT protein efficiently relieves Rb-mediated transcriptional repression. It thus may be more interesting to consider such a mechanism for other interaction partners of truncated LT-Ags, e.g., cellular proteins

that bind to the unique ~110-amino-acid region which precedes the LxCxE region. Another interesting case is that of interaction partners that relocalize to the nucleus when complexed with full-length LT-Ag but fail to do so upon interaction with the truncated protein, such as the lysosomal processing regulator hVam6p (66).

It should also be noted that transformation by cytoplasmic LT-Ags is not without precedent, given that artificially generated mutants of SV40 LT-Ag that fail to localize to the nucleus have been found to be capable of transforming continuously growing rodent cells (67).

In SV40, binding to Rb and p53 contributes to LT protein functions during viral replication and cellular transformation. SV40 LT protein binds directly to the DNA binding domain of p53, thereby suppressing p53-mediated transcriptional activation. The C-terminal domain of LT contains two regions, box 1 and box 2; based on the X-ray structure of SV40 LT in complex with p53, these regions form a single p53 binding site (68). Although amino acids contributing to this particular interaction are not well conserved in MCPyV LT (Fig. 1), earlier experiments using SV40 LT have shown that T-Ag can additionally block p53-dependent transcription and growth arrest by mechanisms that are independent of p53 binding; the N-terminal 121 aa are sufficient to mediate this effect (69, 70). In light of these findings, we have analyzed full-length and truncated MCPyV LT-Ags for their ability to bind to p53 and block p53-dependent transcription. Interestingly, we found that p53-dependent transcription is repressed by full-length MCPyV LT-Ag. Furthermore, we observed that a minor fraction of the protein is in a complex with p53, although significantly less protein coprecipitates p53 than that seen with SV40 LT. Although we cannot fully exclude the possibility that our MCPyV FACS-FRET results were false negative (e.g., due to sterical or structural hindrances), the absence of a signal in this assay together with the poor conservation of residues mediating the contact between SV40 LT-Ag and p53 suggest that a subfraction of MCPyV is complexed with p53 via an indirect interaction. The fact that truncated LT proteins do not coprecipitate p53 suggests that the binding site for such a partner is likely located in a carboxy-terminal region of LT-Ag.

We did not observe an increase in p53 steady-state levels when MCPyV LT full-length protein was expressed, as was recently reported by Li and colleagues (29). Likewise, we were unable to detect increased p21 protein expression or an elevated level of p21, GADD45A, or HDM2 transcription in PFSK-1 or U2OS cells (data not shown). Neither Li et al. nor Cheng et al. (21) observed an interaction between full-length MCPyV LT and p53. At present, we do not have an explanation for these discrepant observations other than the use of different cell lines or experimental approaches. Clearly, however, the results of the three studies are in agreement that shortened MCPyV LT proteins are unable to bind to p53 and interfere with its functions.

Despite their inability to bind to p53, we show here for the first time that the MCC-derived early region expressing a shortened LT can transform primary rodent cells. Similar to data obtained for the BK and JC virus early regions (15–17), however, the efficiency with which these cells were transformed was substantially lower than that for SV40. Likewise, although isolated pBRK cell clones transformed with truncated MCPyV LT proteins do express LT, they do so at significantly lower levels than pBRK cells transformed with SV40 LT. In addition, these cells proliferate much slower than SV40 LT-transformed cells and show a relatively high percentage of apoptotic cells (data not shown), characteristics which have been described for MCC tumor cells (71). It should be pointed out our experiments employ genomic clones that harbor the entire early region from wild-type or MCC-derived MCPyV genomes. These constructs thus should be able to express not only LT but also sT, and it is likely that the sT protein contributes to the transformation events observed in our assays. We have not explicitly tested the transforming potential of sT-deficient LT expression constructs (such constructs would also be expected to yield significantly lower LT levels due to the absence of sT-mediated stabilization of the LT protein). However, given that only constructs encoding truncated LT proteins yield continuously growing colonies in focus formation assays, and since tLT expression furthermore resulted in the outgrowth of larger colonies in anchorage-independent growth assays, our data suggest an important role especially of truncated LT protein during the transformation of primary rodent cells. In contrast to the indirect nature of the p53 interaction, our MST analysis shows that the interaction of MCPyV with Rb is direct and highly efficient. Interestingly, the dissociation constant (K_d) with which a truncated MCPyV LT-Ag bound to the Rb pocket domain indicates an approximately 20-fold-higher binding affinity than that of an N-terminal SV40 fragment (it should be noted that the significance of this observation is presently unclear, given that the SV40 fragment is not a naturally occurring isolate and the full-length protein may exhibit an altered binding affinity). Unfortunately, full-length MCPyV LT-Ag was not efficiently expressed in bacteria, and we were thus unable to directly compare its binding affinity to that of the shortened MCC-derived proteins. Our coimmunoprecipitation experiments together with real-time PCR experiments monitoring E2F-dependent transcription of cdc2 and cyclinA2, however, suggest that the truncated MCC-derived LT-Ag proteins indeed bind more efficiently than the full-length protein. If so, it seems possible that the higher binding affinity may partially compensate for the loss of p53 binding during the transformation process. Clearly, however, under our experimental conditions, under which truncated and full-length LT proteins are ectopically expressed at similar levels, the efficiency with which the shortened proteins led to the derepression of an E2F-regulated reporter was only slightly higher than that for the full-length protein (Fig. 8). Nevertheless, we suspect that, especially for MCC tissues that express LT-Ag at very low or even undetectable levels (25), even small differences in binding affinity may have substantial consequences during the transformation process *in vivo*. Thus, it is conceivable that inhibitors targeting this interaction might be an effective new approach for MCC therapy.

ACKNOWLEDGMENTS

This work was supported by the Structure and Dynamics in Infection graduate school funded by the Federal State Hamburg, Germany.

We are very grateful to Pat Moore and Yuan Chang, University of Pittsburgh, USA, for sending us Cm2B4 antibody. We thank Roland Houben, University Hospital of Würzburg, Germany, for sending us WaGa cells; we thank Franz Oswald, University Hospital Ulm, Germany, for providing the Rb and E2F expression constructs and the pI-H2A-68 luciferase reporter plasmids. Furthermore, we thank Wolfgang Deppert for providing the SV40 plasmid pZIPTEX and the antibody Pab419. We are grateful to Wilhelm Ching for generously providing the p53-CFP/YFP expression constructs. We thank Bernd Zobiak, HEXT, UKE Microscopic Imaging Facility (umif) for help with confocal microscopy.

REFERENCES

1. **DeCaprio JA, Garcea RL.** 2013. A cornucopia of human polyomaviruses. Nat. Rev. Microbiol. **11:**264–276. http://dx.doi.org/10.1038/nrmicro2992.
2. **Korup S, Rietscher J, Calvignac-Spencer S, Trusch F, Hofmann J, Moens U, Sauer I, Voigt S, Schmuck R, Ehlers B.** 2013. Identification of a novel human polyomavirus in organs of the gastrointestinal tract. PLoS One **8:**e58021. http://dx.doi.org/10.1371/journal.pone.0058021.
3. **Feng H, Shuda M, Chang Y, Moore PS.** 2008. Clonal integration of a polyomavirus in human Merkel cell carcinoma. Science **319:**1096–1100. http://dx.doi.org/10.1126/science.1152586.
4. **Becker JC, Houben R, Ugurel S, Trefzer U, Pfohler C, Schrama D.** 2009. MC polyomavirus is frequently present in Merkel cell carcinoma of European patients. J. Invest. Dermatol. **129:**248–250. http://dx.doi.org/10.1038/jid.2008.198.
5. **Busam KJ, Jungbluth AA, Rekthman N, Coit D, Pulitzer M, Bini J, Arora R, Hanson NC, Tassello JA, Frosina D, Moore P, Chang Y.** 2009. Merkel cell polyomavirus expression in Merkel cell carcinomas and its absence in combined tumors and pulmonary neuroendocrine carcinomas. Am. J. Surg. Pathol. **33:**1378–1385. http://dx.doi.org/10.1097/PAS.0b013e3181aa30a5.
6. **Foulongne V, Kluger N, Dereure O, Brieu N, Guillot B, Segondy M.** 2008. Merkel cell polyomavirus and Merkel cell carcinoma, France. Emerg. Infect. Dis. **14:**1491–1493. http://dx.doi.org/10.3201/eid1409.080651.
7. **Garneski KM, Warcola AH, Feng Q, Kiviat NB, Leonard JH, Nghiem P.** 2009. Merkel cell polyomavirus is more frequently present in North American than Australian Merkel cell carcinoma tumors. J. Invest. Dermatol. **129:**246–248. http://dx.doi.org/10.1038/jid.2008.229.
8. **Kassem A, Schopflin A, Diaz C, Weyers W, Stickeler E, Werner M, Zur Hausen A.** 2008. Frequent detection of Merkel cell polyomavirus in human Merkel cell carcinomas and identification of a unique deletion in the VP1 gene. Cancer Res. **68:**5009–5013. http://dx.doi.org/10.1158/0008-5472.CAN-08-0949.
9. **Shuda M, Feng H, Kwun HJ, Rosen ST, Gjoerup O, Moore PS, Chang Y.** 2008. T antigen mutations are a human tumor-specific signature for Merkel cell polyomavirus. Proc. Natl. Acad. Sci. U. S. A. **105:**16272–16277. http://dx.doi.org/10.1073/pnas.0806526105.
10. **Shuda M, Arora R, Kwun HJ, Feng H, Sarid R, Fernandez-Figueras MT, Tolstov Y, Gjoerup O, Mansukhani MM, Swerdlow SH, Chaudhary PM, Kirkwood JM, Nalesnik MA, Kant JA, Weiss LM, Moore PS, Chang Y.** 2009. Human Merkel cell polyomavirus infection I. MCV T antigen expression in Merkel cell carcinoma, lymphoid tissues and lymphoid tumors. Int. J. Cancer **125:**1243–1249. http://dx.doi.org/10.1002/ijc.24510.
11. **Cherington V, Morgan B, Spiegelman BM, Roberts TM.** 1986. Recombinant retroviruses that transduce individual polyoma tumor antigens: effects on growth and differentiation. Proc. Natl. Acad. Sci. U. S. A. **83:**4307–4311. http://dx.doi.org/10.1073/pnas.83.12.4307.
12. **Kornbluth S, Cross FR, Harbison M, Hanafusa H.** 1986. Transformation of chicken embryo fibroblasts and tumor induction by the middle T antigen of polyomavirus carried in an avian retroviral vector. Mol. Cell. Biol. **6:**1545–1551.
13. **Pipas JM.** 2009. SV40: cell transformation and tumorigenesis. Virology **384:**294–303. http://dx.doi.org/10.1016/j.virol.2008.11.024.
14. **Sullivan CS, Pipas JM.** 2002. T antigens of simian virus 40: molecular chaperones for viral replication and tumorigenesis. Microbiol. Mol. Biol. Rev. **66:**179–202. http://dx.doi.org/10.1128/MMBR.66.2.179-202.2002.
15. **Bollag B, Chuke WF, Frisque RJ.** 1989. Hybrid genomes of the polyomaviruses JC virus, BK virus, and simian virus 40: identification of sequences important for efficient transformation. J. Virol. **63:**863–872.
16. **Bollag B, Prins C, Snyder EL, Frisque RJ.** 2000. Purified JC virus T and T′ proteins differentially interact with the retinoblastoma family of tumor suppressor proteins. Virology **274:**165–178. http://dx.doi.org/10.1006/viro.2000.0451.
17. **Dyson N, Bernards R, Friend SH, Gooding LR, Hassell JA, Major EO, Pipas JM, Vandyke T, Harlow E.** 1990. Large T antigens of many polyomaviruses are able to form complexes with the retinoblastoma protein. J. Virol. **64:**1353–1356.
18. **Fischer N, Brandner J, Fuchs F, Moll I, Grundhoff A.** 2010. Detection of Merkel cell polyomavirus (MCPyV) in Merkel cell carcinoma cell lines: cell morphology and growth phenotype do not reflect presence of the virus. Int. J. Cancer **126:**2133–2142. http://dx.doi.org/10.1002/ijc.24877.
19. **Pantulu ND, Pallasch CP, Kurz AK, Kassem A, Frenzel L, Sodenkamp S, Kvasnicka HM, Wendtner CM, Zur Hausen A.** 2010. Detection of a novel truncating Merkel cell polyomavirus large T antigen deletion in chronic lymphocytic leukemia cells. Blood **116:**5280–5284. http://dx.doi.org/10.1182/blood-2010-02-269829.
20. **Arora R, Chang Y, Moore PS.** 2012. MCV and Merkel cell carcinoma: a molecular success story. Curr. Opin. Virol. **2:**489–498. http://dx.doi.org/10.1016/j.coviro.2012.05.007.
21. **Cheng J, Rozenblatt-Rosen O, Paulson KG, Nghiem P, DeCaprio JA.** 2013. Merkel cell polyomavirus large T antigen has growth-promoting and inhibitory activities. J. Virol. **87:**6118–6126. http://dx.doi.org/10.1128/JVI.00385-13.
22. **Asselin C, Gelinas C, Bastin M.** 1983. Role of the three polyoma virus early proteins in tumorigenesis. Mol. Cell. Biol. **3:**1451–1459.
23. **Asselin C, Vass-Marengo J, Bastin M.** 1986. Mutation in the polyomavirus genome that activates the properties of large T associated with neoplastic transformation. J. Virol. **57:**165–172.
24. **Noda T, Satake M, Yamaguchi Y, Ito Y.** 1987. Cooperation of middle and small T antigens of polyomavirus in transformation of established fibroblast and epithelial-like cell lines. J. Virol. **61:**2253–2263.
25. **Shuda M, Kwun HJ, Feng H, Chang Y, Moore PS.** 2011. Human Merkel cell polyomavirus small T antigen is an oncoprotein targeting the 4E-BP1 translation regulator. J. Clin. Invest. **121:**3623–3634. http://dx.doi.org/10.1172/JCI46323.
26. **Houben R, Shuda M, Weinkam R, Schrama D, Feng H, Chang Y, Moore PS, Becker JC.** 2010. Merkel cell polyomavirus-infected Merkel cell carcinoma cells require expression of viral T antigens. J. Virol. **84:**7064–7072. http://dx.doi.org/10.1128/JVI.02400-09.
27. **Kwun HJ, Shuda M, Feng H, Camacho CJ, Moore PS, Chang Y.** 2013. Merkel cell polyomavirus small T antigen controls viral replication and oncoprotein expression by targeting the cellular ubiquitin ligase SCF(Fbw7). Cell Host Microbe **14:**125–135. http://dx.doi.org/10.1016/j.chom.2013.06.008.
28. **Neumann F, Borchert S, Schmidt C, Reimer R, Hohenberg H, Fischer N, Grundhoff A.** 2011. Replication, gene expression and particle production by a consensus Merkel cell polyomavirus (MCPyV) genome. PLoS One **6:**e29112. http://dx.doi.org/10.1371/journal.pone.0029112.
29. **Li J, Wang X, Diaz J, Tsang SH, Buck CB, You J.** 2013. Merkel cell polyomavirus large T antigen disrupts host genomic integrity and inhibits cellular proliferation. J. Virol. **87:**9173–9188. http://dx.doi.org/10.1128/JVI.01216-13.
30. **Graham FL, Smiley J, Russell WC, Nairn R.** 1977. Characteristics of a human cell line transformed by DNA from human adenovirus type 5. J. Gen. Virol. **36:**59–74. http://dx.doi.org/10.1099/0022-1317-36-1-59.
31. **Mitsudomi T, Steinberg SM, Nau MM, Carbone D, D'Amico D, Bodner S, Oie HK, Linnoila RI, Mulshine JL, Minna JD, et al.** 1992. p53 gene mutations in non-small-cell lung cancer cell lines and their correlation with the presence of ras mutations and clinical features. Oncogene **7:**171–180.
32. **Fogh J, Fogh JM, Orfeo T.** 1977. One hundred and twenty-seven cultured human tumor cell lines producing tumors in nude mice. J. Natl. Cancer Inst. **59:**221–226.
33. **Brown TC, Cerutti PA.** 1986. Ultraviolet radiation inactivates SV40 by disrupting at least four genetic functions. EMBO J. **5:**197–203.
34. **Stieler K, Schulz C, Lavanya M, Aepfelbacher M, Stocking C, Fischer N.** 2010. Host range and cellular tropism of the human exogenous gammaretrovirus XMRV. Virology **399:**23–30. http://dx.doi.org/10.1016/j.virol.2009.12.028.
35. **Oswald F, Dobner T, Lipp M.** 1996. The E2F transcription factor activates a replication-dependent human H2A gene in early S phase of the cell cycle. Mol. Cell. Biol. **16:**1889–1895.
36. **Nevels M, Tauber B, Spruss T, Wolf H, Dobner T.** 2001. "Hit-and-run" transformation by adenovirus oncogenes. J. Virol. **75:**3089–3094. http://dx.doi.org/10.1128/JVI.75.7.3089-3094.2001.
37. **Härtl B, Zeller T, Blanchette P, Kremmer E, Dobner T.** 2008. Adenovirus type 5 early region 1B 55-kDa oncoprotein can promote cell transformation by a mechanism independent from blocking p53-activated transcription. Oncogene **27:**3673–3684. http://dx.doi.org/10.1038/sj.onc.1211039.
38. **Wimmer P, Tauber B, Spruss T, Dobner T.** 2010. Adenovirus type 5 early encoded proteins of the E1 and E4 regions induce oncogenic transformation of primary rabbit cells. J. Gen. Virol. **91:**1828–1833. http://dx.doi.org/10.1099/vir.0.020537-0.
39. **Wang X, Li J, Schowalter RM, Jiao J, Buck CB, You J.** 2012. Bromodomain protein Brd4 plays a key role in Merkel cell polyomavirus DNA

replication. PLoS Pathog. **8:**e1003021. http://dx.doi.org/10.1371/journal.ppat.1003021.
40. **Schreiner S, Wimmer P, Groitl P, Chen SY, Blanchette P, Branton PE, Dobner T.** 2011. Adenovirus type 5 early region 1B 55K oncoprotein-dependent degradation of cellular factor Daxx is required for efficient transformation of primary rodent cells. J. Virol. **85:**8752–8765. http://dx.doi.org/10.1128/JVI.00440-11.
41. **Harlow E, Crawford LV, Pim DC, Williamson NM.** 1981. Monoclonal antibodies specific for simian virus 40 tumor antigens. J. Virol. **39:**861–869.
42. **Nevels M, Rubenwolf S, Spruss T, Wolf H, Dobner T.** 1997. The adenovirus E4orf6 protein can promote E1A/E1B-induced focus formation by interfering with p53 tumor suppressor function. Proc. Natl. Acad. Sci. U. S. A. **94:**1206–1211. http://dx.doi.org/10.1073/pnas.94.4.1206.
43. **Hermannstädter A, Ziegler C, Kuhl M, Deppert W, Tolstonog GV.** 2009. Wild-type p53 enhances efficiency of simian virus 40 large-T-antigen-induced cellular transformation. J. Virol. **83:**10106–10118. http://dx.doi.org/10.1128/JVI.00174-09.
44. **Banning C, Votteler J, Hoffmann D, Koppensteiner H, Warmer M, Reimer R, Kirchhoff F, Schubert U, Hauber J, Schindler M.** 2010. A flow cytometry-based FRET assay to identify and analyse protein-protein interactions in living cells. PLoS One **5:**e9344. http://dx.doi.org/10.1371/journal.pone.0009344.
45. **Eward KL, Van Ert MN, Thornton M, Helmstetter CE.** 2004. Cyclin mRNA stability does not vary during the cell cycle. Cell Cycle **3:**1057–1061. http://dx.doi.org/10.4161/cc.3.8.987.
46. **Stieler K, Fischer N.** 2010. Apobec 3G efficiently reduces infectivity of the human exogenous gammaretrovirus XMRV. PLoS One **5:**e11738. http://dx.doi.org/10.1371/journal.pone.0011738.
47. **Leppard KN, Shenk T.** 1989. The adenovirus E1B 55 kd protein influences mRNA transport via an intranuclear effect on RNA metabolism. EMBO J. **8:**2329–2336.
48. **Liu X, Marmorstein R.** 2007. Structure of the retinoblastoma protein bound to adenovirus E1A reveals the molecular basis for viral oncoprotein inactivation of a tumor suppressor. Genes Dev. **21:**2711–2716. http://dx.doi.org/10.1101/gad.1590607.
49. **Jerabek-Willemsen M, Wienken CJ, Braun D, Baaske P, Duhr S.** 2011. Molecular interaction studies using microscale thermophoresis. Assay Drug Dev. Technol. **9:**342–353. http://dx.doi.org/10.1089/adt.2011.0380.
50. **Nakamura T, Sato Y, Watanabe D, Ito H, Shimonohara N, Tsuji T, Nakajima N, Suzuki Y, Matsuo K, Nakagawa H, Sata T, Katano H.** 2010. Nuclear localization of Merkel cell polyomavirus large T antigen in Merkel cell carcinoma. Virology **398:**273–279. http://dx.doi.org/10.1016/j.virol.2009.12.024.
51. **Martin ME, Berk AJ.** 1998. Adenovirus E1B 55K represses p53 activation in vitro. J. Virol. **72:**3146–3154.
52. **Yew PR, Liu X, Berk AJ.** 1994. Adenovirus E1B oncoprotein tethers a transcriptional repression domain to p53. Genes Dev. **8:**190–202. http://dx.doi.org/10.1101/gad.8.2.190.
53. **Bargonetti J, Reynisdottir I, Friedman PN, Prives C.** 1992. Site-specific binding of wild-type p53 to cellular DNA is inhibited by SV40 T antigen and mutant p53. Genes Dev. **6:**1886–1898. http://dx.doi.org/10.1101/gad.6.10.1886.
54. **Harris KF, Christensen JB, Imperiale MJ.** 1996. BK virus large T antigen: interactions with the retinoblastoma family of tumor suppressor proteins and effects on cellular growth control. J. Virol. **70:**2378–2386.
55. **Jiang D, Srinivasan A, Lozano G, Robbins PD.** 1993. SV40 T antigen abrogates p53-mediated transcriptional activity. Oncogene **8:**2805–2812.
56. **Peden KW, Srinivasan A, Farber JM, Pipas JM.** 1989. Mutants with changes within or near a hydrophobic region of simian virus 40 large tumor antigen are defective for binding cellular protein p53. Virology **168:**13–21. http://dx.doi.org/10.1016/0042-6822(89)90398-X.
57. **Peden KW, Srinivasan A, Vartikar JV, Pipas JM.** 1998. Effects of mutations within the SV40 large T antigen ATPase/p53 binding domain on viral replication and transformation. Virus Genes **16:**153–165. http://dx.doi.org/10.1023/A:1007941622680.
58. **Staib C, Pesch J, Gerwig R, Gerber JK, Brehm U, Stangl A, Grummt F.** 1996. p53 inhibits JC virus DNA replication in vivo and interacts with JC virus large T-antigen. Virology **219:**237–246. http://dx.doi.org/10.1006/viro.1996.0241.
59. **Dilworth SM.** 1990. Cell alterations induced by the large T-antigens of SV40 and polyoma virus. Semin. Cancer Biol. **1:**407–414.
60. **Imperiale MJ, Major EO.** 2007. Polyomaviruses, p 2263–2298. *In* Knipe DM, Howley PM, Griffin DE, Lamb RA, Martin MA, Roizman B, Straus SE (ed), Fields virology, 5th ed. Lippincott Williams & Wilkins, Philadelphia, PA.
61. **Wienken CJ, Baaske P, Rothbauer U, Braun D, Duhr S.** 2010. Protein-binding assays in biological liquids using microscale thermophoresis. Nat. Commun. **1:**100. http://dx.doi.org/10.1038/ncomms1093.
62. **Kim HY, Ahn BY, Cho Y.** 2001. Structural basis for the inactivation of retinoblastoma tumor suppressor by SV40 large T antigen. EMBO J. **20:**295–304. http://dx.doi.org/10.1093/emboj/20.1.295.
63. **Tognon M, Corallini A, Martini F, Negrini M, Barbanti-Brodano G.** 2003. Oncogenic transformation by BK virus and association with human tumors. Oncogene **22:**5192–5200. http://dx.doi.org/10.1038/sj.onc.1206550.
64. **Laude HC, Jonchere B, Maubec E, Carlotti A, Marinho E, Couturaud B, Peter M, Sastre-Garau X, Avril MF, Dupin N, Rozenberg F.** 2010. Distinct Merkel cell polyomavirus molecular features in tumour and non tumour specimens from patients with Merkel cell carcinoma. PLoS Pathog. **6:**e1001076. http://dx.doi.org/10.1371/journal.ppat.1001076.
65. **Sastre-Garau X, Peter M, Avril MF, Laude H, Couturier J, Rozenberg F, Almeida A, Boitier F, Carlotti A, Couturaud B, Dupin N.** 2009. Merkel cell carcinoma of the skin: pathological and molecular evidence for a causative role of MCV in oncogenesis. J. Pathol. **218:**48–56. http://dx.doi.org/10.1002/path.2532.
66. **Liu X, Hein J, Richardson SC, Basse PH, Toptan T, Moore PS, Gjoerup OV, Chang Y.** 2011. Merkel cell polyomavirus large T antigen disrupts lysosome clustering by translocating human Vam6p from the cytoplasm to the nucleus. J. Biol. Chem. **286:**17079–17090. http://dx.doi.org/10.1074/jbc.M110.192856.
67. **Zhu J, Rice PW, Gorsch L, Abate M, Cole CN.** 1992. Transformation of a continuous rat embryo fibroblast cell line requires three separate domains of simian virus 40 large T antigen. J. Virol. **66:**2780–2791.
68. **Ahuja D, Saenz-Robles MT, Pipas JM.** 2005. SV40 large T antigen targets multiple cellular pathways to elicit cellular transformation. Oncogene **24:**7729–7745. http://dx.doi.org/10.1038/sj.onc.1209046.
69. **Quartin RS, Cole CN, Pipas JM, Levine AJ.** 1994. The amino-terminal functions of the simian virus 40 large T antigen are required to overcome wild-type p53-mediated growth arrest of cells. J. Virol. **68:**1334–1341.
70. **Rushton JJ, Jiang D, Srinivasan A, Pipas JM, Robbins PD.** 1997. Simian virus 40 T antigen can regulate p53-mediated transcription independent of binding p53. J. Virol. **71:**5620–5623.
71. **Pectasides D, Pectasides M, Economopoulos T.** 2006. Merkel cell cancer of the skin. Ann. Oncol. **17:**1489–1495. http://dx.doi.org/10.1093/annonc/mdl050.
72. **Lilyestrom W, Klein MG, Zhang R, Joachimiak A, Chen XS.** 2006. Crystal structure of SV40 large T-antigen bound to p53: interplay between a viral oncoprotein and a cellular tumor suppressor. Genes Dev. **20:**2373–2382. http://dx.doi.org/10.1101/gad.1456306.